ABSTRACT

Title of Document: INTERFERON GAMMA INDUCIBLE PROTEIN 10 (IP-10) AND REGULATORY T CELLS IN LEISHMANIASIS

Melba Muñoz Roldan, Master of Science, 2007.

Directed By: Professor David M. Mosser
Department of Cell Biology and Molecular Genetics

Leishmania are intracellular parasites that reside inside macrophages and induce weak innate immune responses. We hypothesize that transgenic parasites that express immune response genes could modify the nature of the host response to the parasite. We previously generated transgenic parasites that produce interferon gamma inducible protein 10 (IP-10). C57BL/6 mice are resistant to wild type *L. major* infection but when infected with IP-10 transgenic parasites they develop large lesions in the footpad that do not resolve. Recently it was discovered that nTregs express CXCR3, the receptor for IP-10. We hypothesized that IP-10 transgenic parasites could actively recruit nTregs and thereby enhance parasite persistence. We found higher numbers of $CD4^{+}CD25^{+}Foxp3^{+}$ cells in the draining lymph nodes of IP-10 parasites infected mice compared to wild type infected mice. This work suggests that IP-10 secreting parasites might recruit a population of regulatory T cells that modulates the immune response to the parasite allowing parasite persistence.

INTERFERON GAMMA INDUCIBLE PROTEIN 10 (IP-10) AND REGULATORY T CELLS IN LEISHMANIASIS

By

Melba Lucia Muñoz Roldan

Dissertation submitted to the Faculty of the Graduate School of the
University of Maryland, College Park, in partial fulfillment
of the requirements for the degree of
Master of Science
2007

Advisory Committee:
Professor David Mosser, Chair
Assistant Professor Kenneth Frauwirth
Assistant Professor Volker Briken

Dedication

Siempre pense que el ser humano nunca deberia dejar de soñar y por fortuna yo nunca he dejado de hacerlo. Los sueños por mas irreales que parezcan siempre tienen la posibilidad de convertirse en realidad. Esto lo aprendi de mis padres, los cuales me enseñaron a ver que en la vida no existen los imposibles y que con esfuerzo todo lo que queremos lo podemos lograr. Esta tesis tiene una dedicacion muy especial. Para mis padres amados que me dieron las herramientas necesarias para cumplir mis propositos y para Martin, mi gran amor, que me ha inspirado durante todo este año para realizar mi mayor deseo en este momento.

La vida trae retos a diario y solo cruzando obstaculos podemos seguir creciendo y avanzando en nuestro camino. Esta tesis es la culminacion de mi proyecto de investigacion pero al mismo tiempo es la entrada a un mundo lleno de nuevas oportunidades.

Queridos padres, mi bien del mar, lo mejor esta por venir!

Acknowledgements

I really have no words to express my gratitude to my advisor David Mosser for all his support and everything he has done to help me fulfill my goals. I also want to thank the committee members, Dr. Frauwirth and Dr. Briken for your suggestions and advices for my project. Dalit, thank you for your scientific input, your great suggestions, the valuable advices, your help and guidance for my project but especially for your friendship for a life time. To Sean who generated the parasites for my project and trained me during his last days in the lab, thank you for your guidance and help. Anni, my bench partner, thank you for helping me in the transgenic world of Leishmania. Xia and Shanjin, thank you for your knowledge, for your good suggestions and all your time. Justin, Ron, Zyyan and Bryan, thank you for being good lab mates and answering my questions always with a smile. Ricardo, time has been short but enough to see you are a great guy, good luck in your project.

I also want to thank my dear friends from school. Adri, thank you for your beautiful friendship. You have been like my sister. Te quiero mucho. Joanna, Jess and Amro, thank you for so many moments we shared together and all the memories kept in my heart. To my dear latin lunch group, gracias por los inolvidables almuerzos. Thank you everybody in this department and this program that has touched me in some way.

Table of Contents

List of Tables

List of Figures

Chapter 1: Introduction

Leishmaniasis

Leishmaniasis is a parasitic disease caused by the protozoan *Leishmania*, an obligate intracellular protozoan that resides inside macrophages. It is transmitted by sandfly vectors of the genus *Phlebotomus* and *Lutzomyia* (1). Leishmaniasis causes a spectrum of diseases which can widely vary from a small cutaneous lesion to a life threatening visceral form. The form of the disease depends largely on the parasite species and the immunological status of the host. Leishmaniasis is an increasing health problem mostly in tropical countries where 2 million cases are reported annually with an estimated 12 million people currently infected worldwide (2). In the digestive tract of sand fly vectors, *Leishmania* spp exist as a flagellated, elongated form, called the promastigote. Promastigotes replicate and differentiate into an infectious, non-dividing metacyclic form in the sand fly gut. They are deposited into the skin of the host when sand fly vectors take blood meals. Promastigotes are taken up by macrophages where they differentiate into a non-flagellated, oval-shaped intracellular form, the amastigote. Amastigotes are able to resist the harsh acidic environment of the phagolysosome (3, 4). They replicate inside phagocytes and eventually lyse them. The Leishmania life cycle continues when sand fly vectors take up amastigotes during blood meals. The parasite differentiates into promastigotes in the sand fly gut (5).

The disease Leishmaniasis involves the invasion of macrophages by the parasite and their subsequent intracellular replication. *Leishmania* have evolved several evasion

strategies that allow them to avoid host cellular killing mechanisms. Their survival depends on resisting innate antimicrobial mechanisms of the host and on modulating host adaptive immune responses.

Evasion of the host immune response

Leishmania parasites cause chronic infections in the host to maximize their chances of successful transmission by sand fly vectors. *Leishmania* have evolved a wide variety of host adaptations that allow them to avoid their destruction by the immune system. Parasites can alter their membrane to avoid insertion of lytic C5b-C9 attack membrane complex (6). Promastigotes activate the alternative complement pathway with iC3b and C3b deposition that allows parasite uptake by phagocytes via CR3 and CR1 receptors (7, 8). Opsonic uptake does not activate NADPH oxidase, allowing parasites to enter cells silently. *Leishmania* can also enter macrophages through a silent mechanism similar to the uptake of apoptotic cells (9). In this way they can establish their niche inside macrophages without activating them. Two surface molecules have been implicated in parasite's ingestion, a lipophosphoglycan (LPG) and a surface protease (gp63). LPG promotes intracellular survival of promastigotes by delaying the fusion of the parasite-containing phagosome with the lysosomes (10). Gp63 inhibits degradative phagolysosomal enzymes (11).

Leishmania have also the ability to inhibit protein kinase C (PKC) activation which in turn inhibits phosphorylation at several sites of the signaling pathways that lead to the oxidative burst (12). *Leishmania* cause multiple defects in the induction of cell mediated immunity establishing chronic infections within the host. *Leishmania*

infected macrophages have a reduced class-II-restricted antigen presentation that does not permit efficient T cell activation (13). *Leishmania* infected macrophages are unable to produce IL-12 (14), the main inducer of IFN-γ, a pivotal cytokine for Th1 immune responses against intracellular pathogens. Parasites fail to activate NF-kB, essential in the expression of IL-12 and many other inflammatory cytokines (Mosser lab unpublished data). It has also been observed that Janus-kinases signal transducers and activators of transcription (Jak-STAT) signaling pathways are inhibited in parasite infected macrophages (15).

Using a *Leishmania* model of chronic infection, it has recently been shown that natural T reg cells accumulate at sites of infection (16). It has been suggested that parasites might manipulate regulatory T cells functions by creating an environment that favors their recruitment to the site of infection. In summary, it has been postulated that *Leishmania* are able to evade the host immune responses by inhibiting innate anti-microbial killing pathways in macrophages, enter phagocyte silently, delay phagosome maturation, impair antigen presentation, fail in activating macrophages, and manipulate cells of the adaptive immunity to their benefit to induce long term infections within the host.

Chemokines in Leishmaniasis

Chemokines are a superfamily of small glycoproteins that direct the migration of different types of leukocytes from the blood stream into sites of infection and inflammation. They also play a critical role in allergic responses, infectious and

autoimmune diseases, angiogenesis, inflammation, tumor growth, and hematopoietic development (17, 18). Chemokines are divided into four families based on the location of the two cysteines present in N-terminal portion of the chemokine protein sequence. The four families include the C, CC, CXC, and CX_3C chemokines. They mediate their proinflammatory effects by binding to a variety of specific receptors, belonging to the G protein-coupled superfamily of seven-transmembrane (serpentine) receptors. Chemokines can be produced by a wide variety of cell types in response to pathogen associated molecular patterns found in bacteria, parasites, viruses and danger signals that are released during inflammatory responses (19). Chemokines regulate both the innate and adaptive immunity playing a critical role in the immune response to several pathogens (20).

In humans, leishmaniasis can develop into a self-healing localized cutaneous form (LCL) or a progressive diffuse cutaneous form (DCL). Chemokines might contribute to the development of these different forms of the disease by recruiting different subsets of immune cells to the site of infection. High levels of monocyte chemoattractant protein 1 (MCP-1/CCL2) and interferon-γ inducible protein 10 (IP-10/CXCL10) have been found in skin biopsies from LDL patients (21). In contrast, MIP-1 alpha/CCL3 expression predominates in lesion of DCL patients, where MCP-1 expression is much lower. Recently, an important role of MCP-1 was demonstrated using an experimental model of leishmaniasis. Transgenic MCP-1-secreting parasites are able to recruit restrictive CCR2-positive macrophages to the site of infection.

MCP-1 produced by the transgenic parasites helps to activate CCR2-positive macrophages, making them particularly adept at killing *Leishmania* parasites (22).

There is also evidence that *L. major* downmodulates CCR2 and CCR5 expression in DC and their responsiveness to the respective ligands, CCL2 and CCL3, while enhancing CCR7 expression and the DC response to its ligand CCL21 (23). It might be possible that a different subset of chemokines is expressed among resistant and susceptible mice during leishmaniasis. These chemokines could influence the recruitment of effector cells deciding on the elimination or survival of the parasite. Therefore chemokines are critical key players during the immune response against *Leishmania.* Some of these chemokines and their receptors are shown in Table 1.

IP-10 and Leishmaniasis

Interferon-γ inducible protein, also known as IP-10 or CXCL10, is a CXC chemokine known to bind with high affinity to the CXCR3 receptor expressed on NK cells, CD8+ T-cells, and both CD4+ activated and memory T-cells (24). IP-10 has been shown to attract Th1 polarized cells (25) and is produced by many different cells when activated in response to IFN- γ increasing in turn IFN- γ levels. Previous studies have shown that *L. major* infection upregulates CXCL10 expression in the draining lymph nodes of *L. major*-resistant mice, but not in those of *L. major*-susceptible mice (26).

Family	Chemokine	Receptor	Expression profile of receptor
CC chemokines	MIP-1a, MCP-4, MCP-3, RANTES, MIP-5	CCR1	M, act T, N, Ba, E, D
	MCP-1, MCP-2, MCP-3, MCP-4, MCP-5	CCR2	M, act T, Ba, D, NK
	Eotaxin, Eotaxin-2, Eotaxin-3, MCP-2, MCP-3, MCP-4, RANTES, MIP-5	CCR3	act T, E, Ba, D
	RANTES, MIP-1a, MCP-1	CCR4	act T, Ba, D
	RANTES, MIP-1a, MIP-1b, MCP-2	CCR5	M, act T, D
CXC chemokines	IL-8, GCP-2	CXCR1	N, NK
	IP-10, MIG, ITAC	CXCR3	Act T, NK
CX_3C chemokine	Fracktalkine	CX_3CR1	M, T, NK
C chemokine	Lymphotactin	XCR1	act T, NK

Table 1. Chemokine and their receptors

Chemokines are divided into subfamilies that bind to different classes of receptor expressed on their target cells. Abbreviations: act T, activated T cell; Ba, basophil; D, dendritic cell; E, eosinophil;; M, monocyte; N, neutrophil; NK, natural killer cell; T, T cell.

IP-10 has also been shown to attract natural killer cells (NK) to the site of infection and enhance their cytotoxicity in resistant strains (27). In susceptible mice, the production of IP-10 is much lower and fewer NK cells migrate to the infection site. There is evidence that CCR5 expression in T regs might enable them to preferentially migrate into Leishmania infected sites where they could promote long term survival of the parasite (28).

These studies would suggest a protective role for IP-10 in experimental leishmaniasis. However, the role of IP-10 in immune responses during leishmaniasis is not completely understood. There is evidence that exogenous IP-10 markedly enhances the responsiveness of macrophages to *L. amazonensis* infection. (29). In contrast, other studies have shown that injections of recombinant IP-10 can cause larger lesions in *Leishmania* infected mice (27). Higher IP-10 plasma levels have also been found in patients with visceral leishmaniasis compared to asymptomatic infected individuals, which suggests that IP-10 might play a role in disease exacerbation (30). It has been demonstrated that regulatory T cells express the IP-10 receptor, CXCR3 (31). We hypothesize that IP-10 could recruit a population of regulatory T cells at the draining lymph nodes and sites of infection during leishmaniasis. These regulatory T cells might control Th1 effector cells and enhance *Leishmania* survival.

Regulatory T cells

Regulatory T cells (T regs) are T cells with an immunosuppressive activity that can modulate the immune response and maintain homeostasis. Regulatory T cells can

arise from the natural maturation process in the thymus or be induced in the periphery when exposed to specific stimulatory conditions (32). Several different types of Tregs have been described including naturally arising $CD25^{+}CD4^{+}$ Tregs, IL-10-secreting Tr1 cells, TGF-β-secreting Th3 cells, Qa-1-restricted $CD8^{+}$ T cells, $CD8^{+}CD122^{+}$ T cells, γ/δ T cells, and NKT cells (33-35).

Natural regulatory T cells have been perhaps the most widely studied in human and rodents. They constitutively express CD25, the T cell inhibitory receptor CTLA-4 and the glucocorticoid-inducible tumor necrosis factor receptor (GITR). The transcription factor Foxp3 is required for natural T regs development and is so far the best marker available to identify this cell population (36). Several mechanisms of Treg-mediated suppression have been proposed in the literature. They include direct T cell – T cell interaction involving TGF-β, Lag3, or CTLA-4, perforin and/or granzyme B-dependent killing, IL-10-mediated suppression, modification of the function of dendritic cells, and IL-2 consumption by Tregs. It seems that more than one mechanism of suppression likely operates *in vivo.*

Recently there has been an increased interest in the role of Tregs in infectious diseases and there is evidence that regulatory T cells can prevent clearance of several pathogens (37, 38). Natural regulatory T cells have been found to have not only the ability to recognize self antigens but also to play a critical role in the outcome of microbial infections. They can limit an excessive immune response to pathogens and diminish tissue injury. The difference between natural and induced regulatory T cells

is still not completely clear. Nevertheless, natural regulatory T cells are generally associated with chronic infections which can lead to a detrimental outcome in the host. There are other factors such as the infectious dose, stage of infection and the immunological status of the host that will also influence the result of the interaction between T regs and pathogens.

Natural regulatory T cells and leishmaniasis

After an effective response against pathogens, the immune system needs to limit the inflammatory response; otherwise it will result in tissue damage. Although T regs preserve host homeostasis by controlling excessive immunopathology, they could allow pathogen persistence by controlling effector Th1 cell functions. It has been shown that $CD4^{+}CD25^{+}$ regulatory T cells accumulate at dermal sites of *Leishmania major* infection where they suppress pathogen specific CD4+ T cells (16). Leishmania amazonensis infection model provides an example of the control of immunopathology driven by T regs. The infection is characterized by natural Tregs accumulation at the site of infection which later regulates Leishmania-specific Th1 cells diminishing immunopathology (39). There is also evidence that the transfer of purified natural T regs from an infected donor to a chronically *L. major* infected mouse can result in disease reactivation (40). The mechanisms of how T regs enter sites of infection, is not understood. One possible explanation is the expression of chemokines triggered by parasite for their advantage. The integrin αEβ7 has previously been shown to be expressed at the surface of 25% of the natural Tregs in

lymphoid tissues and all T reg in the dermis of *L. major* infected mice express it (41). The expression of αEβ7 (CD103) is positively regulated by TGF-β (42) and exposure of T cells to *L. major*-infected DCs, suggesting that the parasite itself manipulates its environment to favor Treg retention.

T regs could exert their immunosuppressive functions in an antigen specific manner. It has been shown that T regs proliferate when exposed to *L. major* infected DC and produce high levels of IL-10. This occurs at the site of infection because T regs in other lymphoid organs failed to proliferate in the presence to the antigen (43). This suggests that the parasite has evolved different mechanisms to manipulate DC, which enhance their persistence in the end.

Learning the mechanisms by which natural Tregs are mobilized and activated, and the nature of the antigens they recognize, will be the next step in the design of rational approaches to achieve the appropriate balance between protection and pathology during infections.

CHAPTER 2: MATERIALS AND METHODS

Animal Studies

These studies were reviewed and approved by the University of Maryland Institutional Animal Care and Use Committee. C57BL/6 mice were purchased from Charles River Laboratories (Wilmington, MA)

Parasite culture

Both wild-type and transgenic parasites were grown in 50:50 media [50% Schneider's insect medium (Sigma-Aldrich, St. Louis, MO) supplemented with 20% FBS, 100 U/ml penicillin, 100 µg/ml streptomycin, and 2 mM glutamine and 50% M199 media (Invitrogen, Rockville, MD)]. Transgenic parasites were grown in the presence of 100 µg/ml nourseothricin (SAT) (WERNER BioAgents, Germany).

Parasites, infection, and parasite quantitation

Lesion-derived wild-type and transgenic *L. major* (WHO MHOM/IL/80/Friedlin) were isolated from infected mice as previously described (8). Mice were injected in the right hind footpad with $5x10^5$ wild-type or transgenic stationary *L. major* promastigotes. Lesion size was determined using a caliper to measure the thickness of the infected footpad and subtracting the thickness of the contralateral uninfected footpad as described previously (44). For ear infections, mice were injected in the right and left ears with $1x10^4$ wild-type or transgenic *L. major* parasites. Ear lesion progression was monitored by measuring the diameter of the lesion using an Absolute Digimatic Caliper (Mitutoyo, Ontario, Canada) as previously described (45).

RNA isolation

RNA was isolated from $1x10^8$ wild-type or transgenic *L. major* promastigote using Trizol RNA prep (Invitrogen). The RNA was converted to cDNA using the Invitrogen manufacturer's protocol. Murine IP-10 was amplified from the cDNA samples using the following primers: sense 5'-AAGTGCTGCCGTCATTTTCT-3' and antisense 5'-GTGGCAATGATCTCAACACG-3'. gp63 was amplified using the following primers: sense 5'-ATCCTCACCGACGAGAAGCGCGAC-3' and antisense 5'-ACGGAGGCGACGTACAACACGAAG-3'.

Transgenic IP-10 detection

Costar high-binding ELISA plates (Fisher Scientific) were coated with monoclonal goat anti-mouse IP-10 antibody (capture antibody) from the DuoSet IP-10 ELISA kit (R&D systems, Minneapolis, MN). Wild-type and transgenic parasites ($5x10^6$) were added to the ELISA plate wells for 24 hours. The following day, the parasites were washed away and the IP-10 ELISA was completed according to the manufacturer's protocol using biotinylated anti-mouse IP-10 detection antibody, streptavidin-horseradish peroxidase (HRP), and HRP substrate.

Cytokine measurement

For cytokine analysis, cells from lymph nodes were incubated for 72 h at 37°C, 5% CO_2 at a concentration of 5×10^5 cells in 200 µl RPMI 1640 containing 10% FCS, 10 mM Hepes, L-glutamine, and penicillin/streptomycin in round-bottom 96-well plates in the presence of 20 µg/ml of freeze-thaw *Leishmania* soluble antigen (SLA) prepared from stationary phase promastigotes. IL-10, IFN-γ and IL-4 were measured

from supernatants of SLA stimulated lymphocytes for 72 hours by sandwich ELISA. Capture (clone JESS-2A5) and detection (clone JES513E3) anti-IL-10, capture (clone R4-6A2) and detection (clone XMG1.2) anti-IFN-γ antibodies and capture (clone 11B11) and detection (clone BVD6-24G2) anti-IL-4 antibodies (BD Pharmingen, San Diego, CA) were used.

Isolation of cells from infected mouse ears

Ears infected with wild-type or IP-10 transgenic parasites were excised, soaked in 70% ethanol, and air-dried for 5-10 minutes. The ears were then split into ventral and dorsal portions and placed in liberase (5mg/mL) (Roche, Indianapolis, IN) diluted 1:100 in RPMI for 2 hours at 37 ºC as previously described (45). The ears were put into a 50 μM medicon homogenizer (BD biosciences) with 1 ml PBS and homogenized in BD's Medimachine (BD biosciences) for 2 minutes. The liquefied, homogenized ears were then passed through a 50 μM syringe filcon filter (BD biosciences) and centrifuged at 300g for 10 minutes. The cells isolated from the ears were then resuspended in PBS containing 5% FBS and 5mM EDTA and labeled with antibodies for flow cytometry.

Isolation of cells from Lymph Nodes

Footpad and ears draining lymph nodes were removed from wild type and IP-10 infected C57BL/6 mice at 3, 4, 5, 6 and 7 weeks post infection. Lymph nodes were smashed and passed through a cell strainer, washed with PBS and centrifuged at 300g for 5 minutes. The cells isolated from the ears were then resuspended in PBS containing 5% FBS and 5mM EDTA and labeled with antibodies for flow cytometry.

Flow Cytometry

Cells isolated from ears and lymph nodes were labeled with the following antibodies: PercP-Cy5 conjugated anti-mouse CD4 (clone L3T4) (BD Pharmigen), FITC conjugated anti-mouse CD25 (clone PC61.5), PE conjugated anti-mouse Foxp3 (clone NRRF-30) (eBioscience, San Diego, CA) and PE conjugated anti-mouse CXCR3 (R&D). The isotype controls used were rat IgG2a (eBR2a), rat IgG1 (BD Pharmigen), and rat IgG2b (BD Pharmigen). Before staining, lymph node or dermal cells were incubated with an anti-Fc III/II receptor mAb (2-4G.1) in PBS containing 5% FBS and 5mM EDTA. The staining of surface and intracytoplasmic markers was performed sequentially: the cells were stained first for their surface markers, followed by a permeabilization step and staining for Foxp3. For each sample, 200,000 cells from total were acquired for analysis. The data were collected using CellQuest Pro software (BD Biosciences) and a flow cytometer (FACSCalibur; BD Biosciences). All data was analyzed using FlowJo PC V7.2.1. The lymphocytes from ears and lymph nodes were identified by their CD4 expression.

Intracellular IL-10 staining

To examine IL-10 expression in leukocytes from lymph nodes, we used in vitro restimulation of cells incubated with 10 ng/ml PMA and 500 ng/ml ionomycin for 6 h in the presence of monensin (Golgistop) (BD Bioscience). Stimulated cells were labeled with the following antibodies: PercP-Cy5 conjugated anti-mouse CD4 (clone L3T4), FITC conjugated antimouse CD25 (clone PC61.5) and PE conjugated antimouse IL-10 (clone JES5-16E3) (BD Biosciences and eBioscience, San Diego,

CA). The isotype controls used (all obtained from BD Biosciences) were rat IgG2a (eBR2a), rat IgG1 (R3-34), and rat IgG2b (A-95-1). Staining and analysis was done as described above.

Real-time PCR

Real-time PCR was performed on draining lymph nodes from ear infections. Lymph nodes were passed through a cell strainer and cells were placed into TRIzol. RNA was quantified by spectrophotometry, and cDNA was generated using the ThermoScript kit from Invitrogen according to the manufacturer's instructions. Real-time PCR was performed for IL-10 using the following primer sets from IDT DNA: IL-10 forward, 5'-AAGGACCAGCTGGACAACAT-3'; IL-10 reverse, 5'-TCTCACCCAGGGAATTCAAA-3'; The hypoxanthine phosphoribosyl-transferase (HPRT) gene was used as a housekeeping gene for normalization with the primers 5'-AAGCTTGCTGGTGAAAAGGA-3' (forward) and 5'-TTGCGCTCATCTTAGGCTTT-3' (reverse). Dissociation curves were performed for every run, and data were only analyzed if the curve showed a single peak. Samples from all primer sets were also run on a gel initially to ensure single band products.

rIP-10 injection

For in vivo chemokine treatment, each mouse was injected with recombinant IP-10 (Cedarlane) (100 pg in 30µl containing $5X10^5$ wild type parasites) in the right footpad and a subsequent injection of 1 ng in 10 ul at day 3 post infection.

Chapter 3: DIFFERENCES IN THE PATHOGENICITY OF IP-10 TRANSGENIC AND WILD TYPE PARASITES INFECTED MICE

We hypothesized that a chemokine secreting transgenic parasite would be able to modify the host immune response to the parasite and attract a novel population of immune cells that may have an altered ability to control parasite replication or persistence. IP-10 transgenic infected mice developed a hypervirulent phenotype with larger lesions compared to wild type infected mice. We wanted to confirm differences in the pathogenicity of IP-10 transgenic and wild type parasites using both the footpad and ear model of infection. Subsequently we want to investigate the molecular mechanisms of this observation.

Previous Data

IP-10 secreting parasites were previously generated in our lab (22). C57BL/6 mice are resistant to *Leishmania major* infection. This resistance has been associated with a strong Th1 type cytokine response to the parasite. We had previously demonstrated that C57BL/6 mice infected in the footpad even with a high number of wild type parasites ($5X10^6$) develop lesions that peak between the fourth and the fifth week and then resolve after seven weeks post infection. In contrast C57BL/6 mice infected with IP-10 transgenic *L. major* parasites develop larger lesions. We have shown previously that C57BL/6 mice infected with $5x10^6$ IP-10 transgenic parasites developed large lesions, with the mean swelling of 5.07 ± 0.38 mm on day 31 post-infection (Figure 1A) (Sean Conrad's doctoral thesis, 2006) compared to mice infected with wild-type

L. major, which had a mean peak swelling of 1.83 ± 0.13 mm. This hypervirulent phenotype in C57BL/6 mice infected with transgenic IP-10 parasites correlated with higher number of parasites in the footpad ($5.39x10^8 \pm 3.24x10^8$), local lymph node ($1.1x10^6 \pm 5.6x10^5$), and spleen (6250 ± 551) compared to mice infected with wild-type parasites; foot ($5.93x10^6 \pm 4.8x10^6$), lymph node ($2x10^4 \pm 1.1x10^4$), and spleen (50 ± 9) (Figure 1B).

Current data

Footpad model of infection

Previous work in our lab demonstrated that IP-10 transgenic parasites cause larger lesions in C57BL/6 mice (Sean Conrand's doctoral thesis, 2006). We wished to determine the molecular mechanisms of the difference in pathogenicity between *L. major* wild type and IP-10 transgenic parasite infections in mice.

RNA was extracted during different culture passages of IP-10 transgenic parasites to confirm their IP-10 mRNA expression (Fig 2A). Transgenic parasites expressed IP-10 mRNA in every passage and no expression was detected in wild type parasites as expected. In addition, transgenic *L. major* IP-10 were capable of secreting low levels of IP-10 (35 pg), while the wild-type parasites secreted no IP-10 protein (Fig 2B).

C57BL/6 mice were infected with different amounts of IP-10 transgenic parasites to confirm that hypervirulent phenotype was generated regardless of the number of parasites used for infection. Mice (5 mice per group) were infected in the right

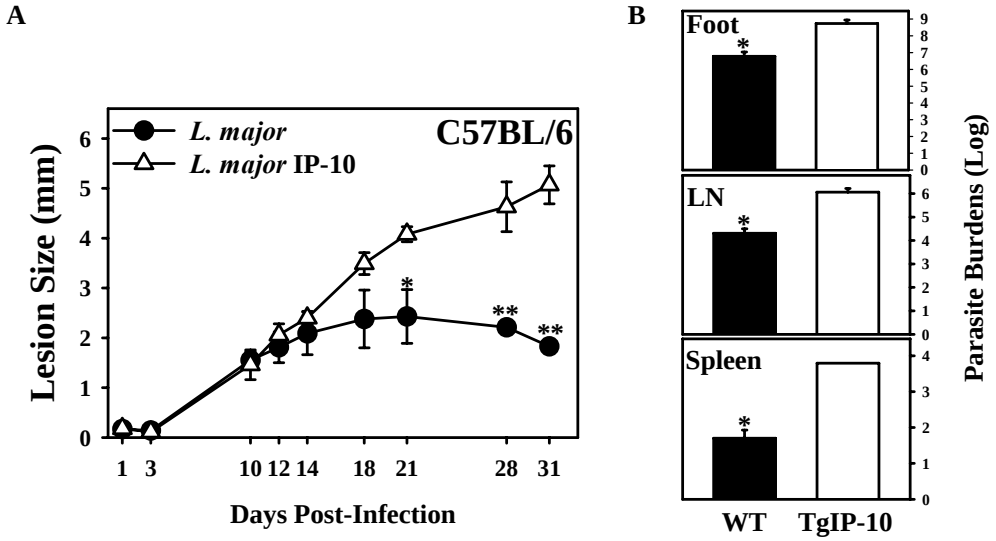

Fig. 1 IP-10 transgenic parasites are hypervirulent

(A) C57BL/6 mice were infected with $5x10^6$ Lm-WT (closed circles) or Lm-TgIP-10 (open triangles) and lesion development was measured at weekly intervals. Parasite burdens were quantitated on day 31 post-infection for C57BL/6 mice infected with Lm-WT (solid bars) and Lm-TgIP-10 (open bars). (Sean Conrad's doctoral thesis, 2006).

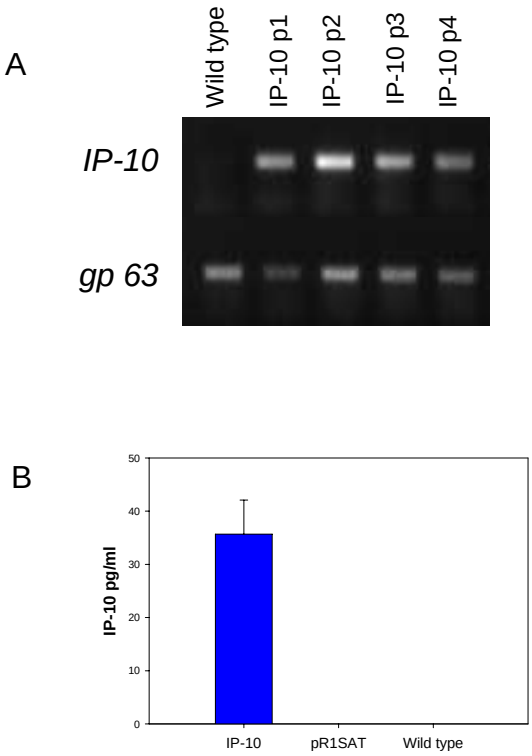

Fig. 2 Transgenic parasites express IP-10 mRNA and protein.

(A) Total RNA was isolated from wild-type and transgenic IP-10 promastigotes. Murine IP-10 was amplified from the cDNA of different culture passages (p) of IP-10 transgenic parasites, but not from the cDNA of wild-type *L. major*. The gene gp63 was amplified from the cDNA as a loading control. (B) A total of $5x10^6$ of IP-10, or wild type parasites were added to ELISA plates coated with monoclonal goat anti-mouse IP-10 antibody. After 24 hours, levels of IP-10 production were determined relative to rIP-10.

footpad with a low dose, $1x10^4$ parasites and then followed for 49 days post infection. IP-10 infected mice developed significantly larger lesions with a mean swelling of 5.3 + 0.7 mm at day 49 post infection ($P < 0.05$). In contrast, wild type infected mice developed lesions with a mean diameter average of 3.63 + 0.16 mm (Fig 3A). Differences in lesion size began to develop by day 21 and lesions from IP-10 transgenic infected mice were significantly larger by day 35 and persisted through day 42 post infection ($P < 0.05$). Using a standard dose of $5x10^5$ parasites, the hypervirulent phenotype was also observed with a mean swelling of 3.8 ± 0.08 mm in the IP-10 transgenic compared to wild type infected mice with a mean swelling of 3.1 ± 0.19 mm at day 28 post infection (Fig 3B). In this case, differences in lesion size was evident by day 21 when lesions from IP-10 transgenic infected mice were already significantly larger and persisted through day 49 post infection ($P < 0.05$).

Ear model of infection

We wanted to reproduce the hypervirulent phenotype of IP-10 transgenic parasites in the ear infection model. This model allows us to more easily isolate cells at the site of infection and analyze differences in cell populations within the lesion. IP-10 transgenic parasites also generated larger lesions compared to wild type infected mice, but this phenotype was not as significant as the one observed in the footpad model. The ear model of infection is technically more challenging compared to the footpad model. It is difficult to accurately inject the small volume of parasites in the ear and to measure small differences in lesion size. Furthermore, lesions in infected ears tend to become necrotic which is also hard to measure. Therefore there is more

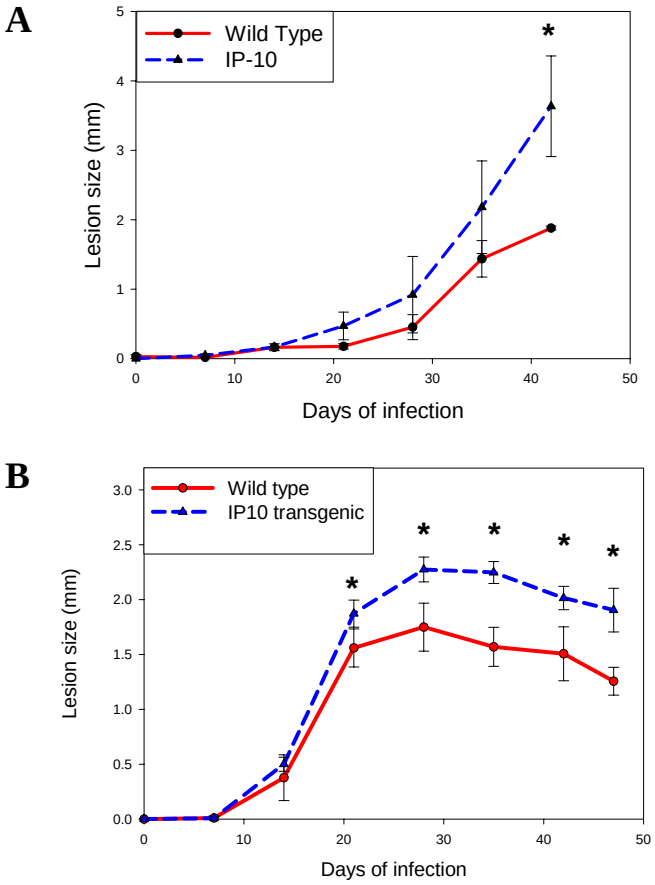

Fig. 3 IP-10 transgenic parasites caused larger lesions in footpads from C57BL/6 mice regardless of parasite dose.

(A) C57BL/6 mice (5 per group) were infected with $1x10^4$ wild type (red line) or IP-10 transgenic parasites (blue line) in the right foot pads and lesion development was measured at weekly intervals for 42 days (*, $p<0.05$) (B) C57BL/6 mice (5 per group) were infected with $5x10^5$ wild type (red line) or IP-10 transgenic parasites (blue line) in the right foot pads and lesion development was measured at weekly intervals for 49 days (*, $p<0.05$).

variability in the phenotype using this model of infection. C57BL/6 mice (3 mice per group) were infected in both ears with $1x10^4$ IP-10 transgenic or wild type parasites. Two experiments were used to compare wild type versus IP-10 parasites phenotype in infected ears. In the first experiment, IP-10 transgenic infected mice had significantly larger ear lesions by day 28 post infection with a mean diameter average of 2.6 ± 0.5 mm compared to wild type infected mice with a mean swelling of 1.33 ± 1 mm ($P < 0.05$) (Fig 4A). Although this difference was significant by day 28, it became smaller at day 35 post infection and the phenotype was not sustained during later time points. In the second experiment, IP-10 transgenic infected mice had a trend towards larger lesions starting at 28 days post infection and persisted through at all later times post infection. There was a significant difference at day 42 post infection when IP-10 transgenic infected mice had a mean diameter average of 3.9 ± 0.4 mm compared to 2.83 ± 0.7 mm in the wild type infected ears ($P < 0.05$) (Fig 4B). The phenotype for the ear model of infection was more variable than the footpad model. This variability may be due to the technical challenges of the model. Therefore we can not conclude from these results that IP-10 trangenic parasite can induce a hypervirulent phenotype in the ears of C57BL/6 mice.

Reconstruction of hypervirulent phenotype in wild type infected mice

We wanted to reconstruct the hypervirulent phenotype observed in footpads of IP-10 infected mice by infecting C57BL/6 mice with wild type parasites along with recombinant IP-10 (rIP-10). Mice (3 per group) were infected in the right footpad with $5x10^5$ wild type, IP-10 transgenic and wild type parasites along with 100 pg of

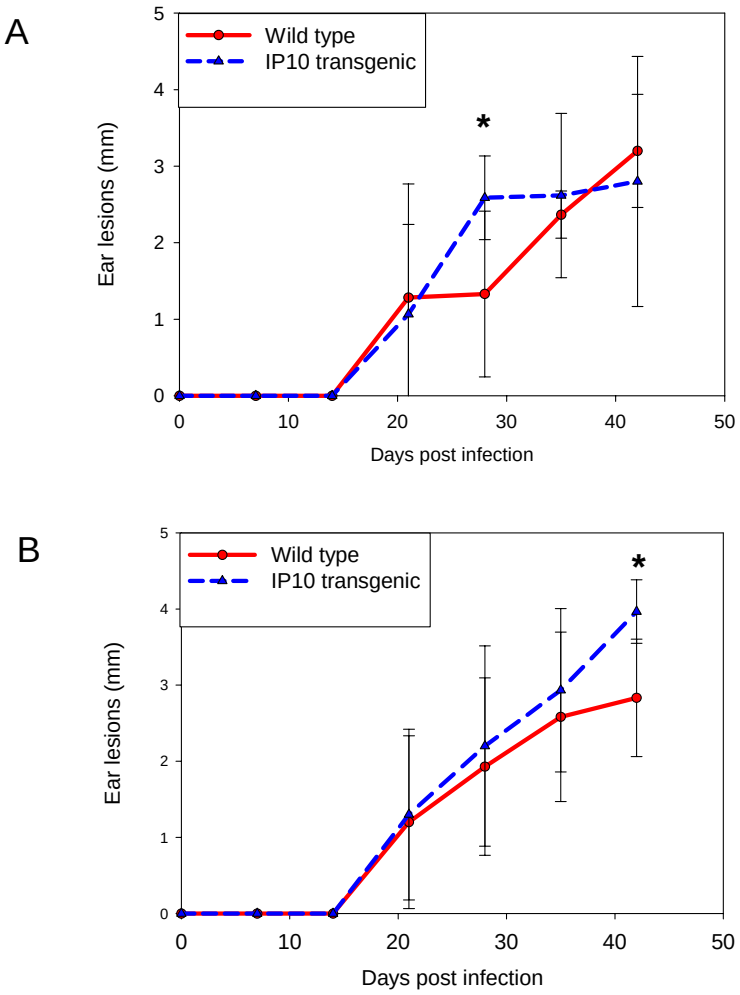

Fig. 4 IP-10 transgenic parasites caused larger lesions in infected ears from C57BL/6 mice.

(A) C57BL/6 mice (3 mice per group) were infected with $1x10^4$ wild type (red line) or IP-10 transgenic parasites (blue line) in both ears and lesion development was measured at weekly intervals for 42 days (*, $p<0.05$.) (B) Second experiment replicate (3 mice per group) with $1x10^4$ wild type (red line) or IP-10 transgenic parasites (blue line) in both ears (*, $p<0.05$).

rIP-10. Lesion development was followed for 35 days post infection. IP-10 infected mice developed significantly larger lesions with a mean swelling of 1.88 ± 0.7 mm at day 35 post infection compared to wild type infected mice with a mean diameter average of 1.15 ± 0.15 mm (Fig 5). Interestingly wild type infected mice that received rIP-10 also developed larger lesions with a mean swelling of 2.1 ± 0.5 mm at day 35 post infection. Wild type infected mice along with rIP-10 injection resembled the hypervirulent phenotype observed in IP-10 transgenic infected mice. This phenotype was identical during 21 days post infection and a more hypervirulent phenotype was observed at latter time points in the group with rIP-10. After day 28 post infection, lesions in wild type infected mice start to plateau but lesions in IP-10 transgenic and wild type along with rIP-10 infected mice were still increasing. IP-10 either secreted by transgenic parasites or injected during footpad infection with wild type parasites caused larger lesions in C57BL/6 mice.

Discussion

This preliminary data shows that IP-10 transgenic parasites cause larger lesions in the footpad model of infection. Regardless of the infection dose, IP-10 transgenic parasites caused a hypervirulent phenotype in *L. major* resistant mice. This finding was consistent in both experiments and we found significant differences between the two groups with larger lesions in IP-10 infected footpads. Results in the ear model were more variable and therefore we can not make the same conclusion. This might have been the result of the higher variability in the ear model. Lesions from *L. major* infected ears tend to last for longer periods of time than footpad lesions in C57BL/6

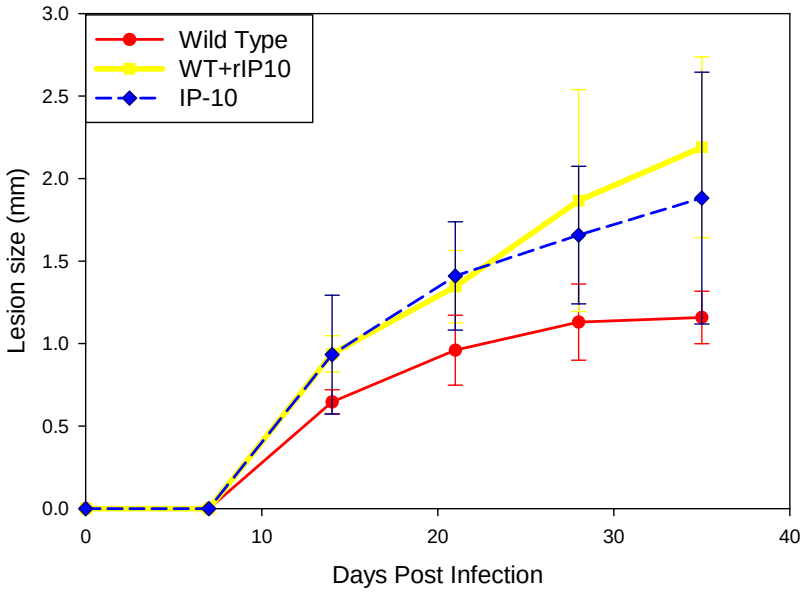

Fig. 5 Reconstruction of hypervirulent phenotype in wild type infected mice.

C57BL/6 mice (3 per group) were infected with $5x10^5$ wild type (red line), IP-10 transgenic parasites (blue line) or wild type with rIP-10 (yellow line) in the right footpad and lesion development was measured at weekly intervals for 35 days.

mice. Differences in pathogenicity could have been more evident in later time points in the ear model. We can not exclude also intrinsic differences between the footpad and the ear model of infection. It might be possible that the infection process is different according to the infection site. Inflammatory cells might be recruited differently in the footpad compared to the ear which might influence the phenotype. We were able to reconstruct the phenotype observed in IP-10 transgenic infection in mice infected with wild type parasites along with an injection of rIP-10. Lesion sizes in mice infected with IP-10 transgenic and rIP-10 injected with wild type parasites were very similar. It seems that both the secreted IP-10 and injected rIP-10 can cause a hypervirulent phenotype in the footpad. Lesions in IP-10 transgenic and rIP-10 injected with wild type infected mice appeared to be increasing during days 28 and 35 post infection when wild type infected mice started to resolve them. This finding suggests that IP-10 can generate larger lesion in mice in the footpad model of infection. From these results we observed that IP-10 transgenic parasites caused more pathology in resistant mice and decided to further investigate this finding.

Chapter 4: MICE INFECTED WITH IP-10 TRANSGENIC PARASITES HAVE HIGHER NUMBERS OF FOXP3^{+} CELLS IN LYMPH NODES COMPARED TO WILD TYPE INFECTED MICE.

Based on differences in the pathogenicity of IP-10 transgenic versus *L. major* wild type parasites in the footpad and ear models of infection, it seems plausible that a chemokine secreting parasites might attract immune cells to the lesion site and draining lymph nodes that could modify the host response. We hypothesized that IP-10 secreting transgenic parasites were able to attract regulatory T cells to the site of infection and local lymph nodes in infected mice. Regulatory T cells express CXCR3, the IP-10 receptor that might allow T cells to migrate preferentially or be retained for longer periods of time at infected dermal sites and draining lymph nodes. Regulatory T cells could control Th1 immune responses, diminishing T helper cells effector functions allowing an enhanced persistence of the parasite. The hypervirulent phenotype could be the result of an increased parasite survival assisted by natural regulatory T cells. If so, this would suggest that parasites might be able to evolve a sophisticated mechanism of using cells of the adaptive immune response to their advantage.

Footpad model of infection

C57BL/6 mice (5 per group) were infected in the right footpad with $5x10^5$ wild type or IP-10 transgenic parasites. Popliteal lymph nodes were removed and cells were isolated at 3, 4, 5 and 6 weeks post infection. Cells from each lymph node of the 5

different infected mice were pooled together and cells were stained for T cells extracellular markers, CD4 and CD25, and the intracellular marker Foxp3, and analyzed by flow cytometry. We used these 3 markers to compare percentages in wild type versus IP-10 infected mice populations of $CD4^+$ $CD25^+$ T cells, $Foxp3^+$ cells from $CD4^+$ $CD25^+$ cells and $CD4^+$ $CD25^+$ $Foxp3^+$ cells (from total population). All data were uniformly analyzed using the same gates in both groups as shown in Fig 6. This figure is an example of how we compared cells percentages between the two groups at each time point post infection. After gating on $CD4^+$ cells, we compared $CD4^+$ $CD25^+$ percentages from wild type (7%) versus IP-10 (7.4%) infected mice. We then compared $Foxp3^+$ cells from the $CD4^+CD25^+$ double positive population, wild type (16.5%) versus IP-10 (23.5%) infected mice. Lastly, we compared $CD4^+$ $CD25^+$ $Foxp3^+$ T cells from the total population from wild type (0.32%) versus IP-10 (0.44%) infected mice. We also compared percentages of $Foxp3^+$ T cells from $CD4^+$ T cells between the two groups. They showed the same pattern as $CD4^+$ $CD25^+$ $Foxp3^+$ cells from total population (data not shown). We hypothesized that mice infected with IP-10 parasites will recruit higher numbers of $Foxp3^+$ cells from $CD4^+$ $CD25^+$ cells and $CD4^+$ $CD25^+$ $Foxp3^+$ T cells from total populations of lymph nodes compared to wild type infected mice.

We found similar numbers of $CD4^+$ $CD25^+$ T cells in both IP-10 and wild type infected mice and only at day 21 the percentage of $CD4^+$ $CD25^+$ T cells in IP-10 transgenic was slightly higher (9.7%) than in wild type mice (8.1%). At day 28 we found the opposite, wild type infected mice had a higher percentage of $CD4^+$ $CD25^+$

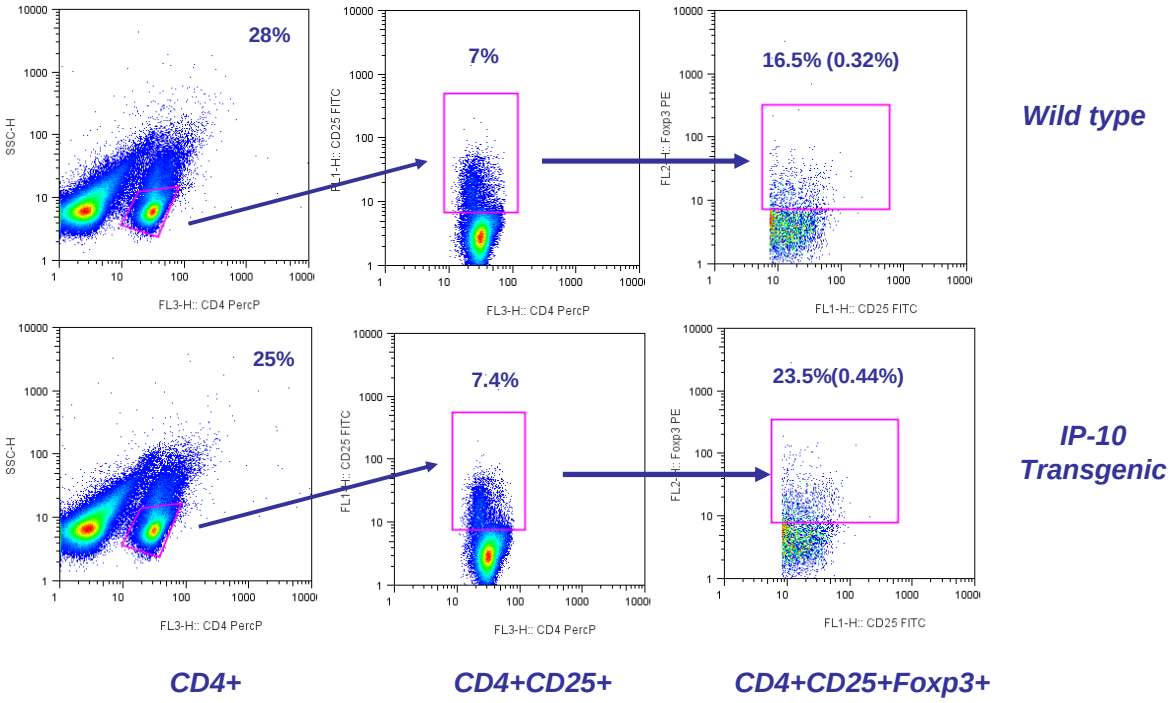

Fig. 6 Flow cytometry analysis in lymph nodes

C57BL/6 mice were infected in the right footpad with $5x10^5$ wild type (top) or IP-10 transgenic (bottom) parasites. Popliteal lymph nodes were removed and cells from each lymph node were pooled and stained for CD4, CD25 and Foxp3 markers. All data were analyzed using the same gates. In this example from day 35 post infection, we compared $CD4^+$ $CD25^+$ percentages from wild type (7%) versus IP-10 (7.4%) infected mice. We then compared $Foxp3^+$ cells from the $CD4^+CD25^+$ double positive population, wild type (16.5%) versus IP-10 (23.5%) infected mice. Lastly, we compared $CD4^+$ $CD25^+$ $Foxp3^+$ T cells from the total population from wild type (0.32%) versus IP-10 (0.44%) infected mice.

T cells (12.5%) compared to IP-10 infected mice (8.5%) (Fig. 7A). Differences in the percentage of $Foxp3^+$ cells from $CD4^+$ $CD25^+$ cells were fairly small, 12.8% and 11.4% in IP-10 transgenic and wild type mice respectively (Fig 7B) at day 21 post infection. At day 28 post infection, percentages of $Foxp3^+$ cells from $CD4^+$ $CD25^+$ T cells and $CD4^+$ $CD25^+$ $Foxp3^+$ cells were slightly higher in wild type infected mice. Nevertheless, we observed a dramatic increase in the percentage of $Foxp3^+$ T cells (15.2%) from $CD4^+CD25^+$ population (or 0.21% from total population) in lymph nodes from IP-10 transgenic infected mice compared to 5.9% (or 0.06% from total population) at day 42 post infection (Fig. 7B and 7C). It seems that IP-10 secreting parasites are able to attract $CD4^+CD25^+Foxp3^+$ cells to the draining lymph nodes in infected mice after 5 weeks post infection and this recruitment becomes significant at 6 weeks post infection. During early stages of infection, we did not observe an evident difference in the number of $Foxp3^+$ cells between wild type and IP-10 transgenic infected mice. Nevertheless, there was a considerable difference at day 42 post infection between the two groups. These results might suggest that IP-10 transgenic parasites could recruit $Foxp3^+$ cells at late stages of infection.

Ear model of infection

Analysis of lesion sites

C57BL/6 mice (3 mice, 6 ears and lymph nodes per group) were infected in both ears with $1x10^4$ wild type and IP-10 transgenic parasites. Cells were isolated from the lesions and lymph nodes from infected mice in two experiment replicates. Cells from

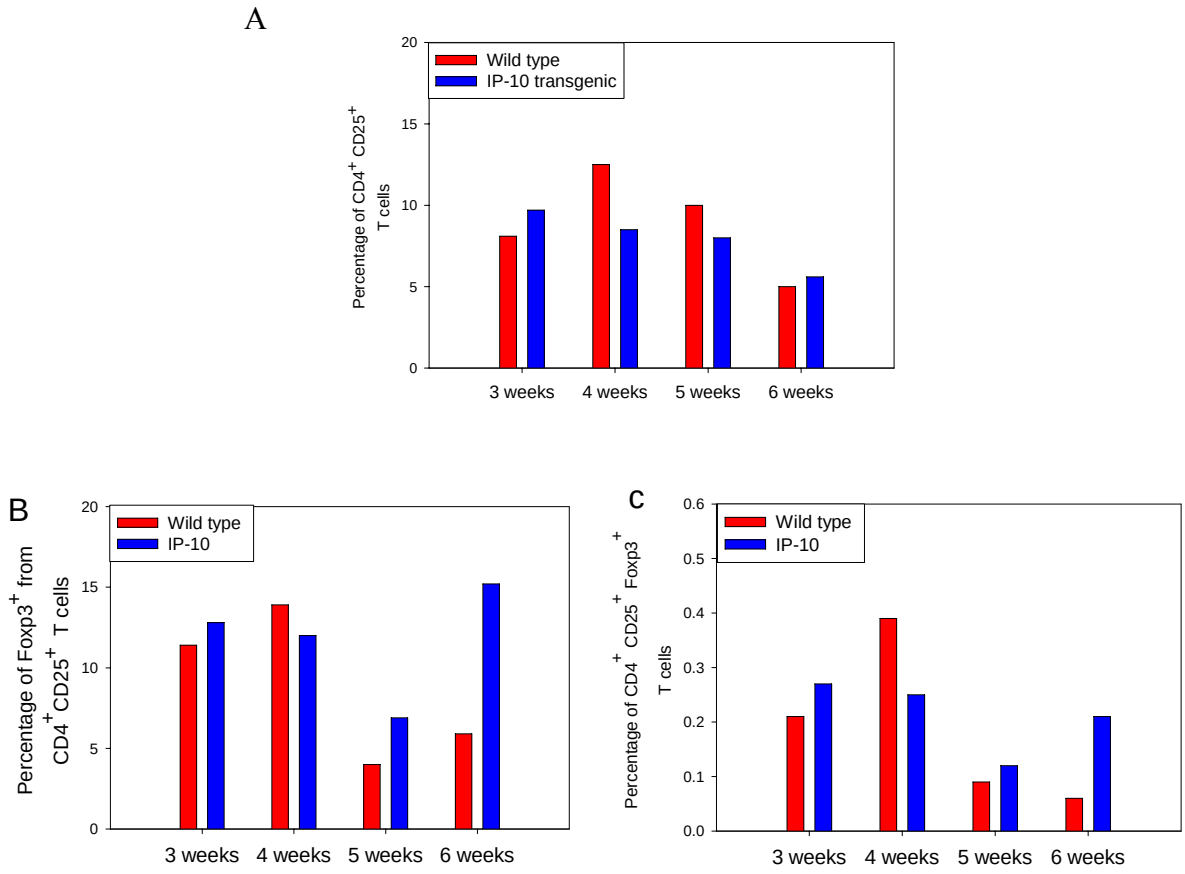

Fig 7 Higher Foxp3$^+$ cells were found in the popliteal lymph nodes from mice infected with IP-10 transgenic parasites at late stages of infection.

C57BL/6 mice (5 per group) were infected in the right footpad with 5x10^5 wild type (red bars) or IP-10 transgenic (blue bars) parasites. Popliteal lymph nodes were removed at 3, 4, 5 and 6 weeks post infection and cells were stained for CD4, CD25 and Foxp3 markers. Percentages of CD4$^+$ CD25$^+$ T cells (A), Foxp3$^+$ cells from CD4$^+$ CD25$^+$ cells (B) and CD4$^+$ CD25$^+$ Foxp3$^+$ cells (from total population) (C) were compared between IP-10 transgenic and wild type infected mice by flow cytometry analysis.

infected ears were isolated, pooled and stained for the same markers used in the footpad model of infection. All data were uniformly analyzed using the same gates as shown in Fig 8. This figure is an example of how we compared cells percentages between the two groups at each time point post infection. After gating in $CD4^+$ cells, we compared $CD4^+$ $CD25^+$ percentages from wild type (17.4%) versus IP-10 (18.9%) infected mice. We then compared $Foxp3^+$ cells from the $CD4^+CD25^+$ double positive population, wild type (12.5%) versus IP-10 (17.5%) infected mice. Lastly, we compared $CD4^+$ $CD25^+$ $Foxp3^+$ T cells from the total population from wild type (0.05%) versus IP-10 (0.04%) infected mice.

In the first experiment, we found comparable numbers of $CD4^+CD25^+$ cells in lesions from IP-10 transgenic and wild type infected mice except at day 35 post infection when we observed a higher percentage in the wild type (18.3%) compared to IP-10 (11.2%) infected ears. However this difference was reversed at day 42 post infection when we found 12.8% of $CD4^+CD25^+$ cells in the IP-10 compared to 9.7% in the wild type lesions (Fig. 9A). We also observed higher percentages of $Foxp3^+$ T cells from $CD4^+CD25^+$ cells in IP-10 transgenic infected mice from lesions at 4, 5 and 6 weeks post infection. The largest difference was observed at day 35 with 11.8% of $Foxp3^+$ cells from $CD4^+CD25^+$ cells in IP-10 transgenic infected ears compared to 4.3% in the wild type (Fig. 9B and 9C). There was a similar trend in both IP-10 and wild type infected ears showing the highest percentage of $CD4^+CD25^+$ and $Foxp3^+$ cells from $CD4^+CD25^+$ T cells at day 28 post infection with a progressive decline in cell

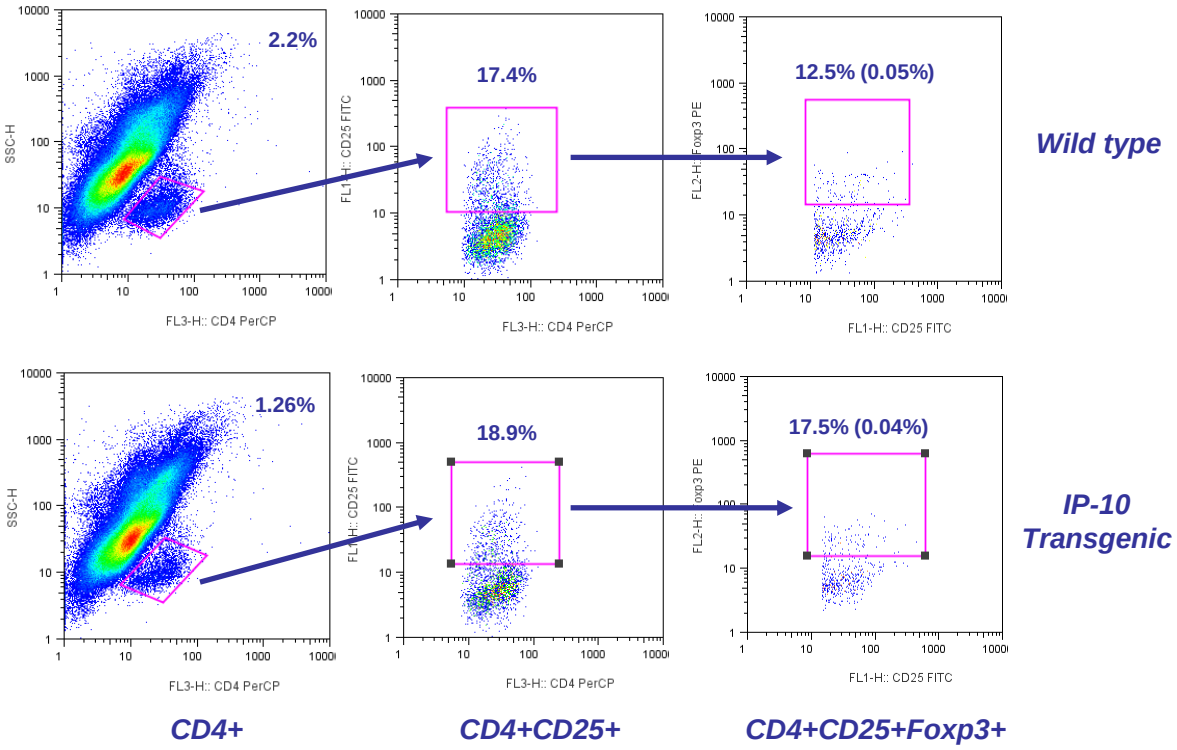

Fig. 8 Flow cytometry analysis in lesions from ears

C57BL/6 mice were infected in both ears with $1x10^4$ wild type (top) or IP-10 transgenic (bottom) parasites. Cells were removed, pooled and stained for CD4, CD25 and Foxp3 markers. All data were analyzed using the same gates. This figure is an example of how we compared percentages between the two groups at each time point post infection. In this example from day 28 post infection, we compared $CD4^+$ $CD25^+$ percentages from wild type (17.4%) versus IP-10 (18.9%) infected mice. We then compared $Foxp3^+$ cells from the $CD4^+CD25^+$ double positive population, wild type (12.5%) versus IP-10 (17.5%) infected mice. Lastly, we compared $CD4^+$ $CD25^+$ $Foxp3^+$ T cells from the total population from wild type (0.05%) versus IP-10 (0.04%) infected mice.

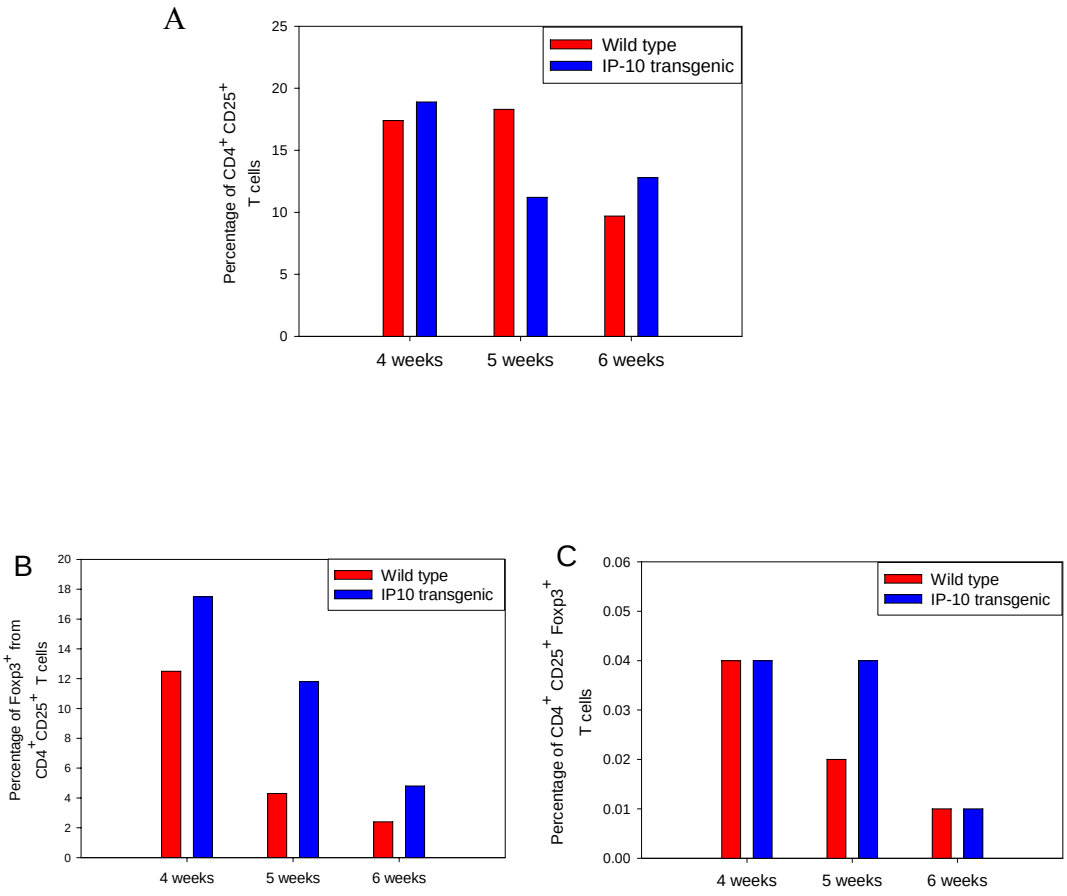

Fig. 9 Higher Foxp3$^+$ cells were found in the lesions from mice infected with IP-10 transgenic parasites. (First experiment)

C57BL/6 mice (3 per group) were infected in both ears with 1x10^4 wild type (red bars) or IP-10 transgenic parasites (blue bars). Cells were isolated from infected ears at 4, 5 and 6 weeks post infection and stained for CD4, CD25 and Foxp3 markers. Percentages of CD4$^+$ CD25$^+$ T cells (A), Foxp3$^+$ cells from CD4$^+$ CD25$^+$ cells (B) and CD4$^+$ CD25$^+$ Foxp3$^+$ cells (from total population) (C) were compared between IP-10 transgenic and wild type infected mice by flow cytometry analysis.

numbers from this time point until day 42 post infection. In this first experiment we observed more $Foxp3^+$ cells in the IP-10 transgenic group than in the wild type infected one, especially evident after 5 weeks post infection. IP-10 secreting parasites might be able to actively recruit natural regulatory T cells at the site of infection. Nevertheless we only observed a tendency of higher numbers of $Foxp3^+$ cells in the IP-10 transgenic infected ears in this model of infection. There was a 3 fold difference at day 35 post infection between the two groups. Whether this finding is a direct consequence of IP-10 acting needs to be further assessed.

In the second experiment, there were more $CD4^+$ $CD25^+$ cells in the IP-10 infected ears after 4, 5 and 6 weeks post infection. Differences were more evident at 4 and 5 weeks post infection with 24% versus 18.5% and 16% versus 10.8% from IP-10 transgenic and wild type infected ears respectively (Fig. 10A). Percentages of $CD4^+CD25^+Foxp3^+$ cells from total population were similar in IP-10 transgenic and wild type infected mice from lesions after 4 and 5 weeks post infection (Fig. 10B). However, there was a clear difference in the number of $CD4^+CD25^+Foxp3^+$ cells at day 42 post infection in the IP-10 infected mice (0.02% from total population) with no $CD4^+CD25^+Foxp3^+$ cells found at this time point in wild type infected ears (Fig. 10B). Differences in this second experiment were not consistent with the previous experiment. We observed higher numbers of $Foxp3^+$ cells at the lesions of mice infected with IP-10 parasites only at day 42 post infection in the second experiment whereas the difference between groups was more evident at day 35 post infection in

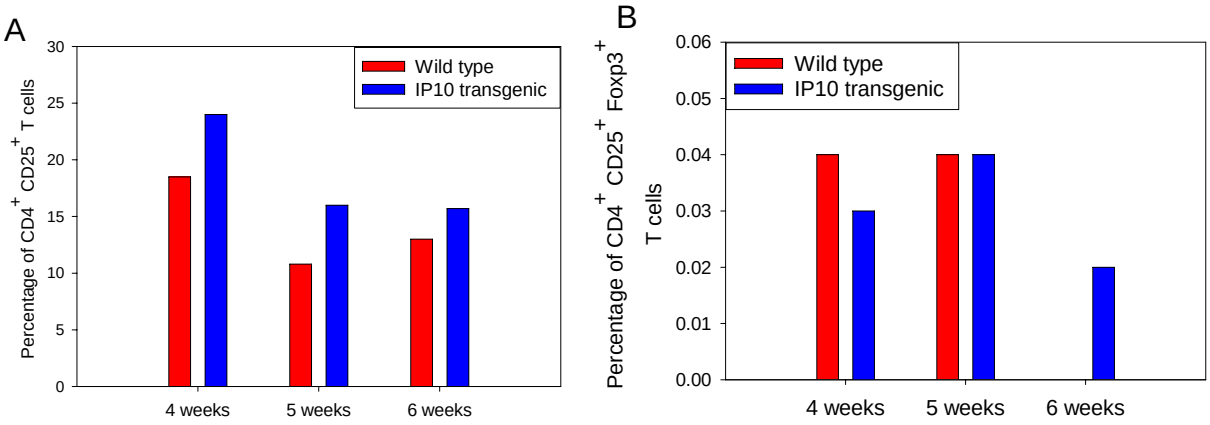

Fig. 10 Higher Foxp3$^+$ cells were found in the lesions from mice infected with IP-10 transgenic parasites at late stages of infection. (Second experiment)

C57BL/6 mice (3 per group) were infected in both ears with 1x10^4 wild type (red bars) or IP-10 transgenic (blue bars) parasites. Cells were isolated from infected ears at 4, 5 and 6 weeks post infection and stained for CD4, CD25 and Foxp3 markers. Percentages of CD4$^+$ CD25$^+$ T cells (A), Foxp3$^+$ cells from CD4$^+$ CD25$^+$ cells (B) and CD4$^+$ CD25$^+$ Foxp3$^+$ cells (from total population) (C) were compared between IP-10 transgenic and wild type infected mice by flow cytometry analysis

the first experiment. These discrepancies might be related to the variability observed in the phenotype in the two experiments (Fig 4). However the higher number in $Foxp3^+$ cells at day 42 post infection correlates with the significant larger lesion in IP-10 transgenic infected mice found in the second experiment. It might be possible that larger differences occurred after 42 days post infection. These results can only suggest a trend of higher numbers of $Foxp3^+$ cells in infected ears with IP-10 transgenic parasites compared to wild type parasites.

Analysis of draining lymph nodes

Cells from retromaxillar lymph nodes of infected mice were also isolated and analyzed by flow cytometry using the same markers. In the first experiment, percentages of $CD4^+CD25^+$ cells were higher in lymph nodes from IP-10 compared to wild type infected mice. This difference was more evident at day 28 post infection (Fig. 11A). We also found higher percentages of $Foxp3^+$ cells from $CD4^+CD25^+$ cells in lymph nodes from IP-10 transgenic compared to wild type infected mice after 4 and 5 weeks post infection. The largest difference was observed at day 35 post infection when the percentage of $Foxp3^+$ cells from $CD4^+CD25^+$ cells in IP-10 infected mice was 8.1% compared to 3% in the wild type infected mice (Fig. 11B and 11C). At day 42 post infection, percentages of $Foxp3^+$ cells from $CD4^+CD25^+$ cells in IP-10 and wild type infected mice were not significantly different. These results correlate well with the results from the first experiment in the lesion sites where the largest difference in the number of $Foxp3^+$ cells from $CD4^+CD25^+$ cells in IP-10 transgenic mice was also observed at day 35 post infection.

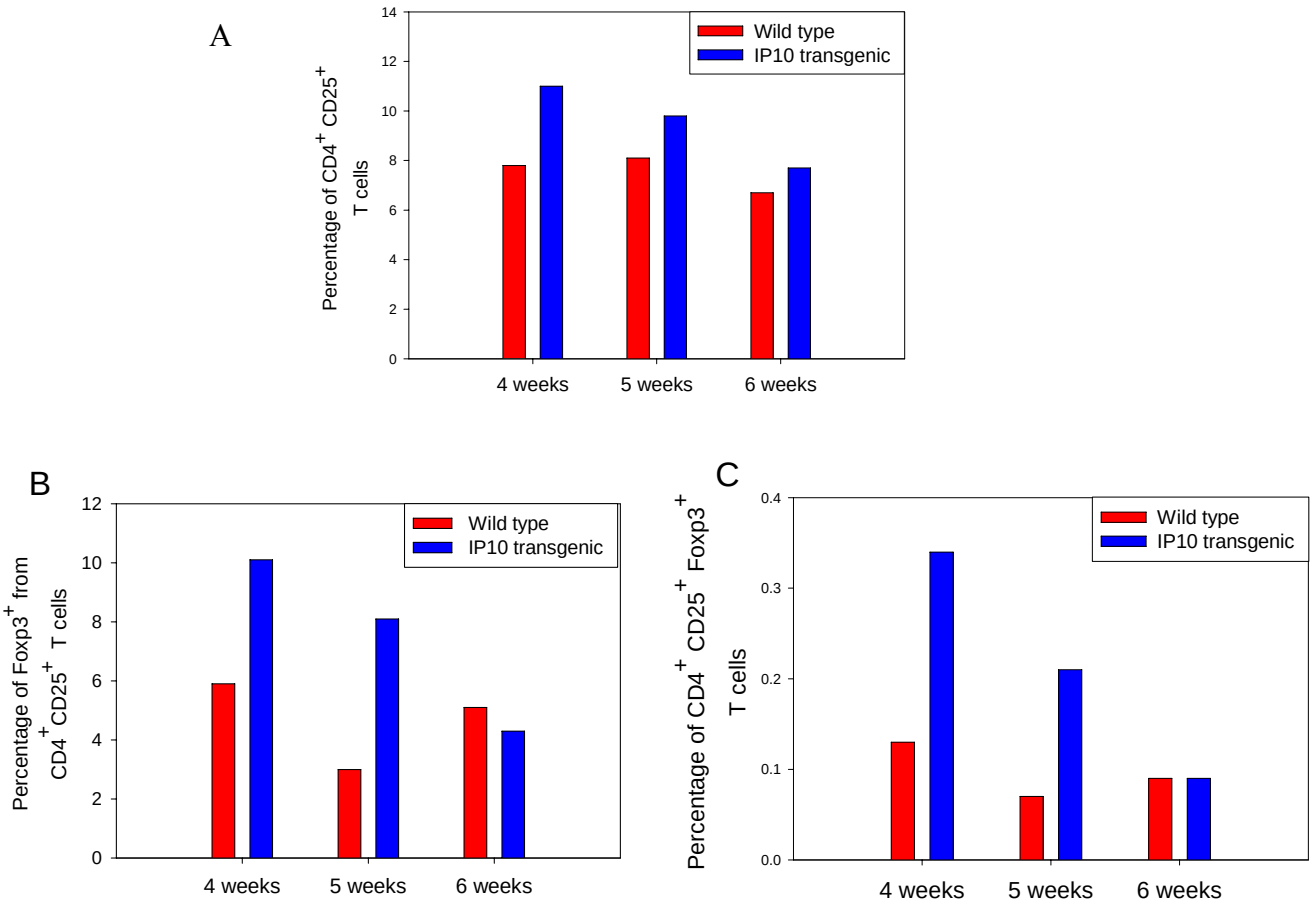

Fig. 11 Higher Foxp3$^+$ cells are found in retromaxillar lymph nodes from mice infected with IP-10 transgenic parasites. (First experiment)

C57BL/6 mice (3 per group) were infected in both ears with 1x10^4 wild type (red bars) or IP-10 transgenic (blue bars) parasites. Retromaxillar lymph nodes were removed at 4, 5 and 6 weeks post infection and cells were stained for CD4, CD25 and Foxp3 markers. Percentages of CD4$^+$ CD25$^+$ T cells (A), Foxp3$^+$ cells from CD4$^+$ CD25$^+$ cells (B) and CD4$^+$ CD25$^+$ Foxp3$^+$ cells (from total population) (C) were compared between IP-10 transgenic and wild type infected mice by flow cytometry analysis.

In the second experiment, percentages of $CD4^+CD25^+$ cells in lymph nodes from IP-10 and wild type infected mice were similar, except at day 42 post infection when we observed 10.5% in the IP-10 compared to 7.5% in the wild type (Fig. 12A). However, we also found higher percentages of $Foxp3^+$ cells from $CD4^+CD25^+$ cells in IP-10 transgenic compared to wild type infected mice after 3, 4 and 5 weeks of infection. Differences were more evident at day 28 post infection with 30.3% in the IP-10 compared to 22% in the wild type (Fig. 12B and 12C). Percentages of $CD4^+CD25^+Foxp3^+$ cells became comparable in both groups by day 42 post infection.

Analysis of $CXCR3^+$ cells in popliteal lymph nodes

CXCR3 is the receptor of IP-10 expressed in T cells and NK cells. Both activated $CD4^+CD25^+$ T cells and regulatory T cells express it. We found similar numbers of $CD4^+CD25^+$ T cells, or activated T cells in both IP-10 transgenic and wild type infected mice but higher numbers of $Foxp3^+$ cells were observed in mice infected with IP-10. We wanted to assess CXCR3 expression in lymph nodes from infected mice in both groups. We hypothesize that lymph nodes from mice infected with IP-10 parasites could have higher CXCR3 expression which might correlate with higher number of natural regulatory T cells found in IP-10 transgenic mice. We infected C57BL/6 mice (3 per group) with $5x10^5$ parasites in the right footpad. Cells from popliteal lymph nodes were pooled and stained for T cells extracellular markers, CD4 and CD25 and CXCR3 and analyzed by flow cytometry.

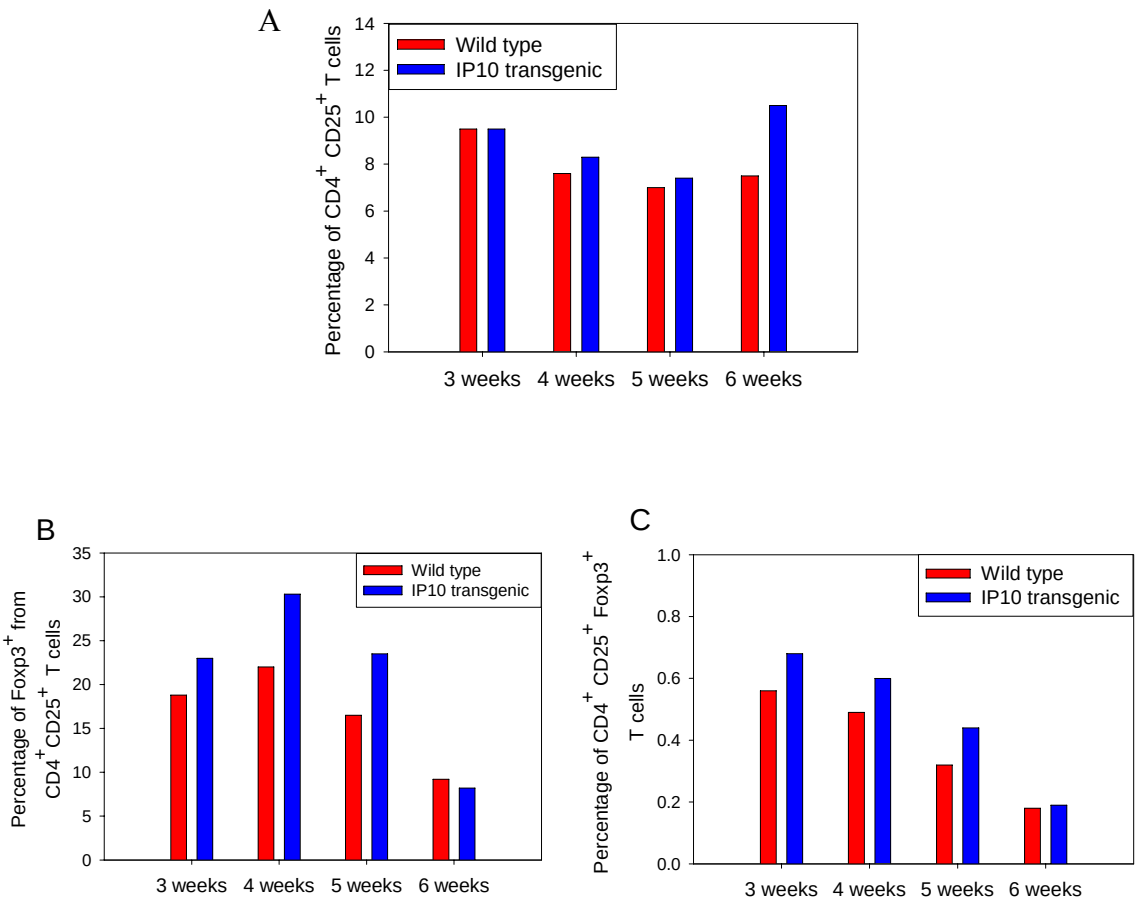

Fig. 12 Higher Foxp3$^+$ cells are found in retromaxillar lymph nodes from mice infected with IP-10 transgenic parasites. (Second experiment)

C57BL/6 mice (3 per group) were infected in both ears with 1x10^4 wild type (red bars) or IP-10 transgenic (blue bars) parasites. Retromaxillar lymph nodes were removed at 4, 5 and 6 weeks post infection and cells were stained for CD4, CD25 and Foxp3 markers. Percentages of CD4$^+$ CD25$^+$ T cells (A), Foxp3$^+$ cells from CD4$^+$ CD25$^+$ cells (B) and CD4$^+$ CD25$^+$ Foxp3$^+$ cells (from total population) (C) were compared between IP-10 transgenic and wild type infected mice by flow cytometry analysis.

We found comparable numbers of activated T cells, $CD4^+CD25^+$ T cells in both group at weeks 3, 4 and 5 post infection (Fig 13A). However we observed slightly higher numbers of $CD4^+CD25^+CXCR3^+$ T cells in lymph nodes from mice infected with IP-10 transgenic mice compared to wild type parasites at days 21, 28 and 35 post infection (Fig 13B). Although there were similar numbers of activated T cells in both groups, these results might suggest that IP-10 transgenic parasites could recruit higher numbers of natural regulatory T cells to the draining lymph nodes with higher expression of CXCR3 and Foxp3 markers.

Discussion

These results show that IP-10 transgenic infected mice recruit higher numbers of $CD4^+CD25^+Foxp3^+$ cells to the lesion sites and their draining lymph nodes compared to wild type infected mice. This seems to be a late event in footpad infections and an earlier event in the ear model of infection. A higher percentage of $Foxp3^+$ cells was found at day 42 post infection in the foot pad model of infection while in the ear model was found between day 28 and 35. Higher numbers of $Foxp3^+$ cells were found in both ears and retromaxillar lymph nodes in the first experiment. We observed a 3 fold increase in the percentage of $Foxp3^+$ cells from $CD4^+CD25^+$ cells in the draining lymph nodes of infected ears at day 35 post infection. Results were also consistent between the first and the second experiments from retromaxillar lymph nodes of

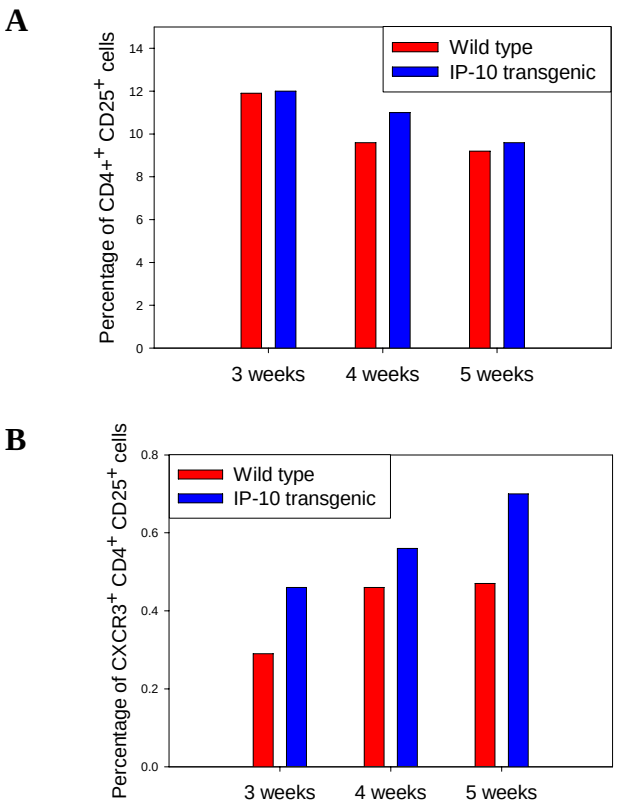

Fig. 13 Higher CXCR3$^+$ cells are found in the popliteal lymph nodes from mice infected with IP-10 transgenic parasites.

C57BL/6 mice (3 per group) were infected in the right footpad with 5x10^5 wild type (red bars) or IP-10 transgenic (blue bars) parasites. Lymph nodes were removed at 3, 4, and 5 weeks post infection and cells were stained for CD4, CD25 and CXCR3 markers. Percentages of CD4$^+$ CD25$^+$ T cells (A) and CD4$^+$ CD25$^+$ CXCR3$^+$ cells (B) were compared between IP-10 transgenic and wild type infected mice by flow cytometry analysis.

infected mice. There were higher numbers of $Foxp3^+$ cells during weeks 4 and 5 post infection in both experiments. Results were less consistent between ear experiments; however higher numbers of $Foxp3^+$ cells were also found but at different time points post infection. Higher numbers of $Foxp3^+$ cells from $CD4^+CD25^+$ cells were found in ear lesions at weeks 4 and 5 post infection in the first experiment and at week 6 in the second one. Although there were not dramatic differences between IP-10 transgenic and wild type infected mice, we observed a similar trend in all experiments. Higher numbers of $Foxp3^+$ cells were found in IP-10 transgenic mice compared to wild type infected mice. This might suggest that IP-10 parasites could recruit or retain regulatory T cells in these areas and the hypervirulent phenotype could result from natural regulatory T cells immunosuppressive responses.

We also found higher expression of CXCR3 in draining lymph nodes from IP-10 infected mice. There was a correlation in the expression of Foxp3 and CXCR3 in lymph nodes from infected footpads. Higher numbers of $Foxp3^+$ cells and $CXCR3^+$ were found after day 35 postinfection. It might be plausible that IP-10 actively recruits or retains for longer periods natural regulatory T cells at the draining lymph nodes. These cells which express more Foxp3 and CXCR3 might enhance *L. major* survival in resistant mice and cause a hypervirulent phenotype.

Chapter 5: CYTOKINE EXPRESSION PATTERNS IN DRAINING LYMPH NODES OF WILD TYPE VERSUS IP-10 TRANSGENIC INFECTED MICE.

We found higher numbers of $CD4^+CD25^+Foxp3^+$ cells at the dermal sites and draining lymph nodes in IP-10 transgenic infected mice compared to the wild type after 4, 5 and 6 weeks post infection. Both the footpad and ear models of infection showed higher numbers of $Foxp3^+$ cells in IP-10 infected mice. We wanted to identify and compare the cytokine expression in lymph node cells from these infected mice. We hypothesized that regulatory T cells that migrated or are retained longer at draining lymph nodes have high IL-10, but low IFN-γ and low IL-4 expression. Higher percentages of $CD4^+CD25^+IL\text{-}10^+$ cells might be found in IP-10 transgenic infected mice and these might correlate with higher numbers of $Foxp3^+$ cells found in lymph nodes and lesions. We used the ear model of infection to assess IL-10 expression in retromaxillar lymph nodes at 3, 4, 5 and 6 weeks post infection by flow cytometry. Intracellular staining was performed in PMA and ionomycin stimulated cells in vitro and the percentages of $IL\text{-}10^+$ cells from $CD4^+CD25^+$ and $CD4^+CD25^+IL\text{-}10^+$ cells from total population were compared between IP-10 and wild type infected mice. All flow data was uniformly analyzed and the same gates were used to assess $CD4^+CD25^+IL\text{-}10^+$ cells as illustrated in fig 14. This figure is an example of how we compared cells percentages between the two groups at each time point post infection. After gating on $CD4^+$ cells, we compared $CD4^+$ $CD25^+$ percentages from wild type (6.5%) versus IP-10 (7.4%) infected mice. We then

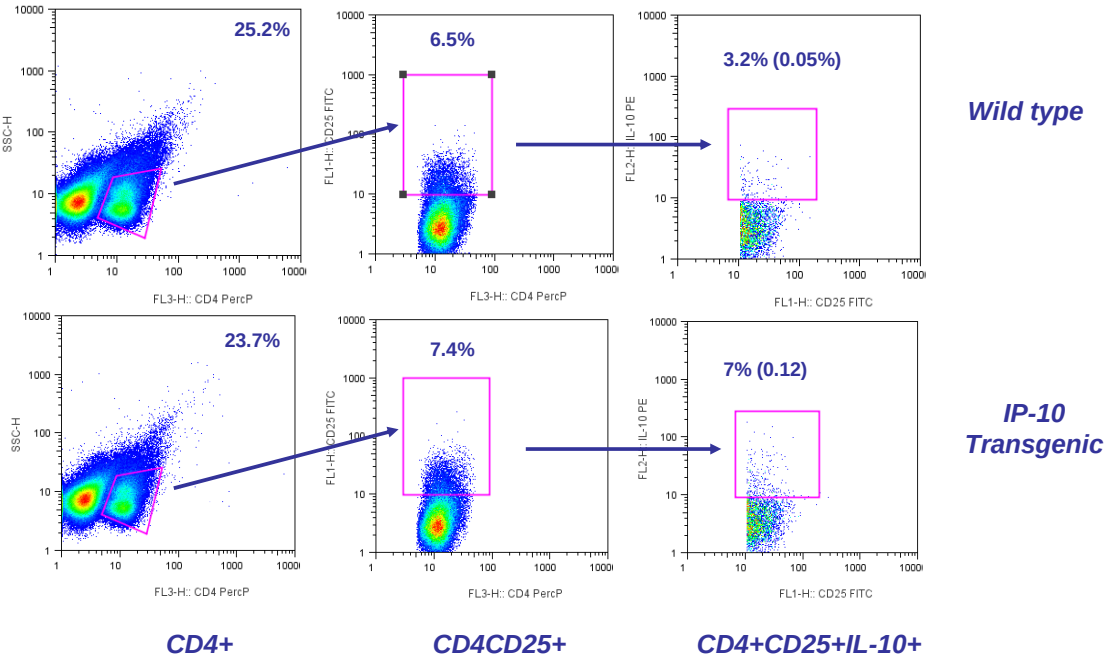

Fig. 14 IL-10 intracellular staining in lymph nodes

Retromaxillar lymph nodes were removed and cells from lymph nodes were pooled and stained for CD4, CD25 and IL-10. All data were analyzed using the same gates. This figure is an example of how we compared cells percentages between the two groups at each time point post infection. In this example from day 42 post infection, we compared $CD4^+$ $CD25^+$ percentages from wild type (6.5%) versus IP-10 (7.4%) infected mice. We then compared $IL\text{-}10^+$ cells from the $CD4^+CD25^+$ double positive population, wild type (3.2%) versus IP-10 (7%) infected mice. Lastly, we compared $CD4^+$ $CD25^+$ $IL\text{-}10^+$ T cells from the total population from wild type (0.05%) versus IP-10 (0.12%) infected mice.

compared IL-10^+ cells from the $CD4^+CD25^+$ double positive population, wild type (3.2%) versus IP-10 (7%) infected mice. Lastly, we compared $CD4^+$ $CD25^+$ IL-10^+ T cells from the total population from wild type (0.05%) versus IP-10 (0.12%) infected mice. We assessed IL-10 expression in two separate experiments.

In the first experiment, we observed an increased percentage of IL-10^+ cells from $CD4^+CD25^+$ cells in retromaxillar lymph nodes from IP-10 transgenic infected mice compared to the wild type infected mice at every time point post infection. The highest number of IL-10^+ cells was found after 4 weeks post infection, with 4% in the IP-10 infected mice compared to 2.8% in the wild type (Fig. 15A and 15B). In the second experiment, we observed the highest percentage of IL-10^+ cells from $CD4^+CD25^+$ and $CD4^+CD25^+$IL-10^+ cells at 6 weeks post infection, with 3.2% of IL-10^+ cells in the wild type compared to 7% in IP-10 transgenic infected mice (Fig. 16A and 16B). These results correlate well with the higher number of $CD4^+CD25^+Foxp3^+$ cells found draining lymph nodes of IP-10 transgenic infected mice. Higher numbers of natural regulatory T cells found in mice infected with IP-10 transgenic parasites might exert their immunosuppressive functions through an IL-10 dependent mechanism.

We also measured IL-10, INF-γ and IL-4 expression by ELISA from supernatants of soluble leishmania antigen (SLA) stimulated cells for 72 hours. We used both the footpad and the ear models of infection to assess cytokine expression in lymph nodes from IP-10 and wild type infected mice. In the footpad group we found higher levels

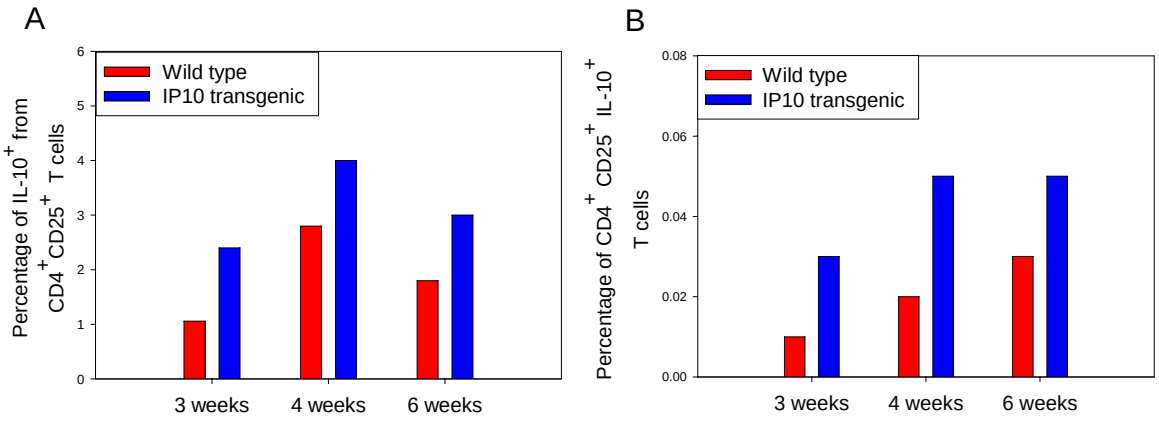

Fig. 15 Higher IL-10$^+$ cells were found in retromaxillar lymph nodes from IP-10 transgenic infected mice. (First experiment)

C57BL/6 mice (3 per group) were infected in both ears with 1x10^4 wild type (red bars) or IP-10 transgenic (blue bars) parasites. Retromaxillar lymph nodes were removed at 3, 4 and 6 weeks post infection and cells were stained for CD4, CD25 and IL-10 markers. Percentages IL-10$^+$ cells from CD4$^+$ CD25$^+$ cells (A) and CD4$^+$ CD25$^+$ IL-10$^+$ cells (from total population) (B) were compared between IP-10 transgenic and wild type infected mice by flow cytometry analysis

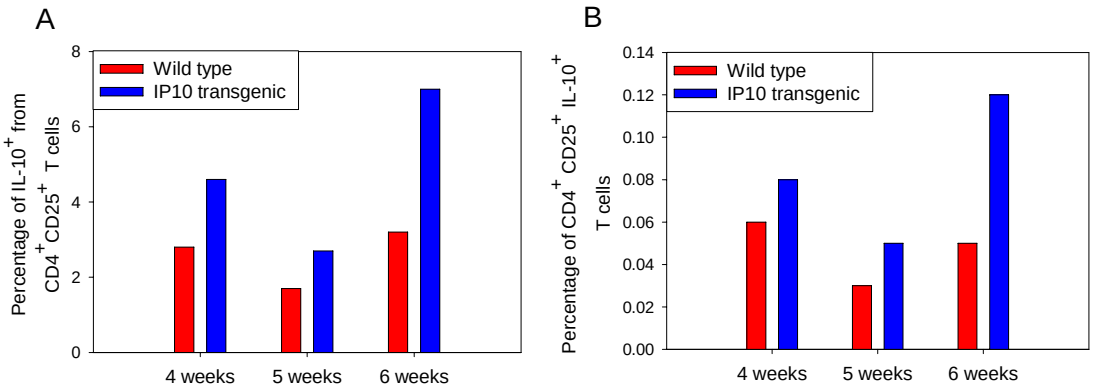

Fig. 16 Higher IL-10$^+$ cells were found in retromaxillar lymph nodes from IP-10 transgenic infected mice. (Second experiment)

C57BL/6 mice (3 per group) were infected in both ears with 1x10^4 wild type (red bars) or IP-10 transgenic (blue bars) parasites. Retromaxillar lymph nodes were removed at 4, 5 and 6 weeks post infection and cells were stained for CD4, CD25 and IL-10 markers. Percentages IL-10$^+$ cells from CD4$^+$ CD25$^+$ cells (A) and CD4$^+$ CD25$^+$ IL-10$^+$ cells (from total population) (B) were compared between IP-10 transgenic and wild type infected mice by flow cytometry analysis.

of IL-10 at day 21 post infection from the popliteal lymph node in the IP-10 infected mice (Fig. 17A). This difference became less evident at day 28 and at day 35 when levels of IL-10 were the same in both IP-10 and wild type infected mice. IFN-γ levels followed a similar pattern with higher levels in the IP-10 infected mice at day 21 but similar levels at day 28 and 35 post infection (Fig. 17B). IL-4 was only detected at 21 days post infection in the wild type infected group and no expression was detected for the IP-10 infected mice. No IL-4 was detected at later time points (Fig. 17C).

Using the ear model of infection we isolated cells from retromaxillar lymph nodes and stimulated them with SLA for 72 hours. We found higher IL-10 expression at day 35 and 42 post infection in the IP-10 compared to wild type infected mice (Fig. 18A). No differences were found in IFN-γ expression at day 35 post infection between both groups and levels were very low (Fig. 18B). However, IFN-γ expression was significantly higher in wild type infected mice at day 42 post infection compared to IP-10 transgenic infected mice. IL-4 expression was low in general. This is to be expected in C57BL/6 mice which induce a Th1 response to these parasites. There was higher IL-4 in the wild type infected mice at day 35 post infection, with no detectable levels in the IP-10 infected mice. The opposite was observed at day 42 post infection when low levels of IL-4 were detected in IP-10 infected mice and no levels were detected in wild type (Fig. 18C).

We also examined cytokine induction in draining lymph nodes from IP-10 and wild type infected mice by RT-PCR. We used the ear model of infection and isolated mRNA from lymph nodes. Cells were harvested into TRIzol and in vivo cytokine

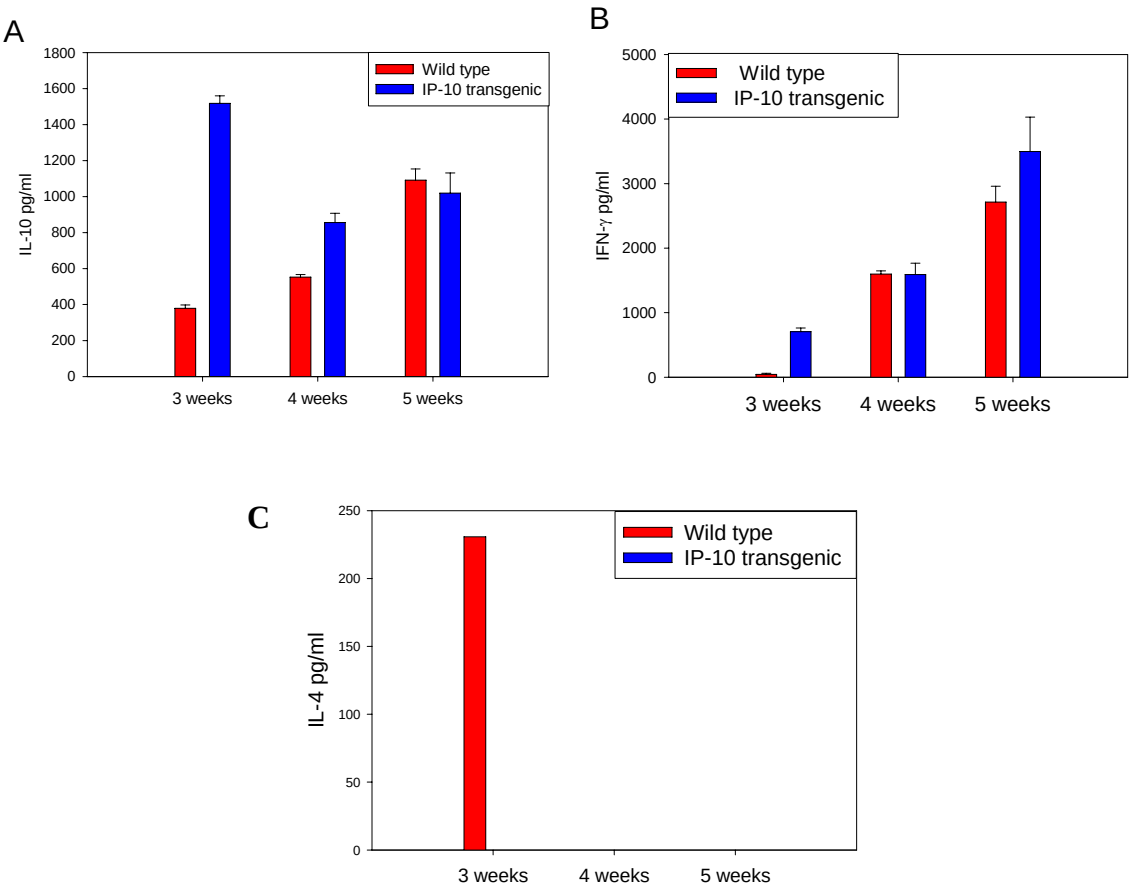

Fig. 17 Cytokine expression in lymph nodes from IP-10 transgenic and wild type infected footpads.

Popliteal lymph nodes were incubated for 72 h at 37°C, 5% CO_2 at a concentration of 5 x 10^5 cells in 200 µl of RPMI 1640 containing 10% FCS, 10 mM Hepes, L-glutamine, and penicillin/streptomycin in round-bottom 96-well plates in the presence of 20 µg/ml of freeze-thawed *Leishmania* antigen prepared from stationary phase promastigotes. IL-10 (A), IFN-γ (B) and IL-4 (C) were measured from supernatants of SLA stimulated lymphocytes for 72 hours by sandwich ELISA.

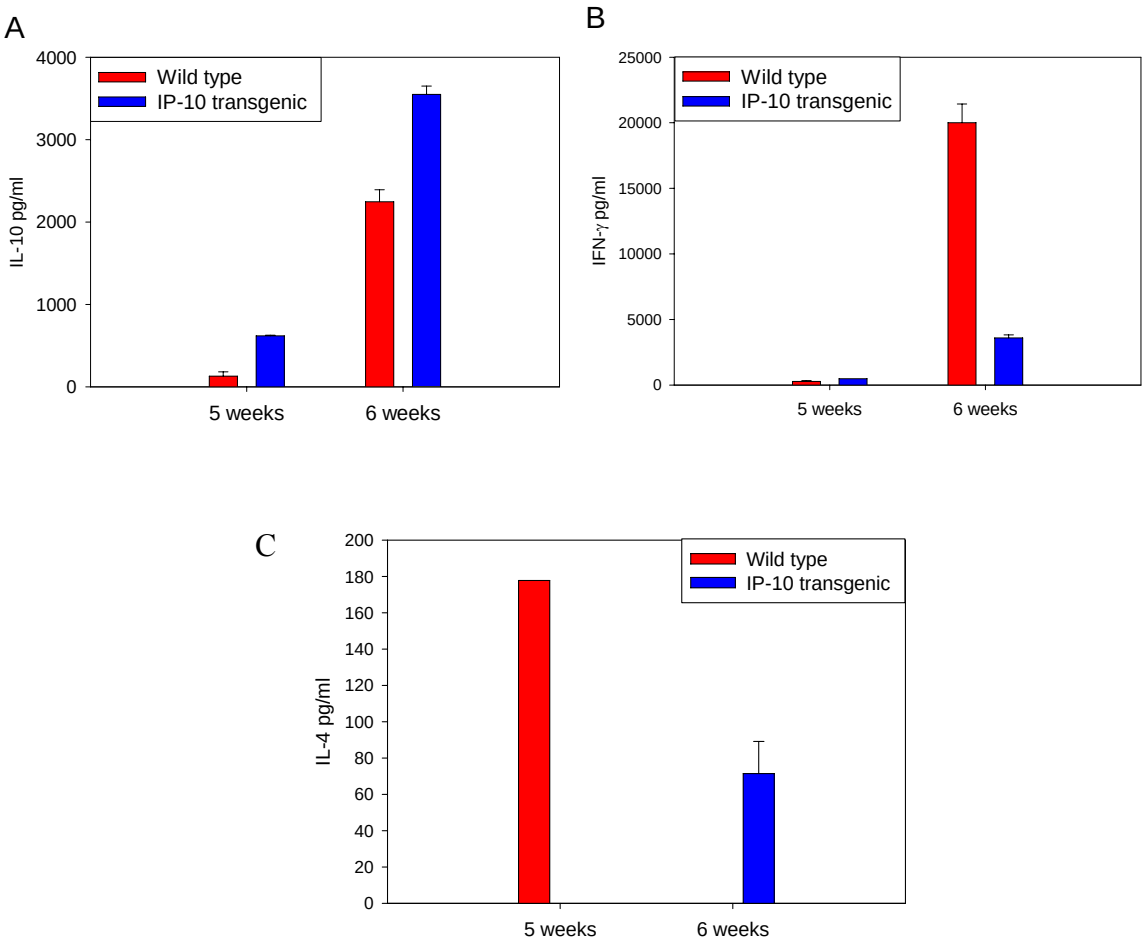

Fig. 18 Cytokine expression in retromaxillar lymph nodes from IP-10 transgenic and wild type infected mice.

Retromaxillar lymph nodes were incubated for 72 h at 37°C, 5% CO_2 at a concentration of 5 x 10^5 cells in 200 µl of RPMI 1640 containing 10% FCS, 10 mM Hepes, L-glutamine, and penicillin/streptomycin in round-bottom 96-well plates in the presence of 20 µg/ml of freeze-thawed *Leishmania* antigen prepared from stationary phase promastigotes. IL-10 (A), IFN-γ (B) and IL-4 (C) were measured from supernatants of SLA stimulated lymphocytes for 72 hours by sandwich ELISA.

mRNA levels were determined using real-time PCR and normalized to HPRT. Data are expressed as relative changes (fold) compared to uninfected lymph nodes, which were normalized to 1. We detected very low levels of mRNA IL-10 expression in both wild type and IP-10 infected mice. IP-10 transgenic parasites induced slightly more IL-10 mRNA than wild type parasites at 4 and 5 weeks post infection (Fig. 19A).

Discussion

These results showed that IP-10 transgenic infected mice had higher numbers of $CD4^{+}CD25^{+}IL\text{-}10^{+}$ cells in the draining lymph nodes compared to the wild type infected mice. Higher numbers of $IL\text{-}10^{+}$ cells were found at day 28, 35 and 42 post infection in IP-10 infected mice when higher numbers of $Foxp3^{+}$ cells were also found. This might suggest that natural regulatory T cells that are recruited to draining lymph nodes in infected mice, express IL-10 and this could in part enhanced parasite survival. We also found higher numbers of $IL\text{-}10^{+}$ cells at the lesion sites in the ears which also correlates with higher numbers of $Foxp3^{+}$ cells (data not shown). Higher IL-10 expression was also found in the supernatants of SLA stimulated cells from IP-10 infected mice at day 35 and 42 post infection in draining lymph nodes from infected ears. There were very small IL-10 relative fold changes in cells from both infected groups compared to uninfected lymph nodes detected by RT-PCR. We observed slightly higher IL-10 mRNA expression in lymph nodes from mice infected with IP-10 transgenic parasites than wild type parasites. There was only one relative

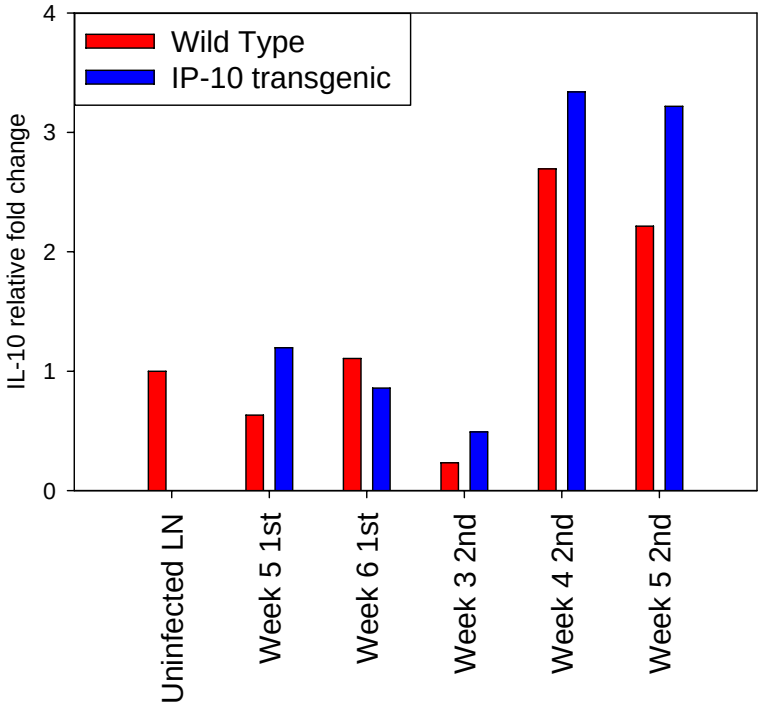

Fig. 19 Cytokine induction by RT-PCR

Real-time PCR was performed for IL-10 on draining lymph nodes from mice infected in both ears. Cells were placed into TRIzol and RNA was quantified by spectrophotometry. cDNA was generated using the ThermoScript kit from Invitrogen according to the manufacturer's instructions. In vivo cytokine mRNA levels were determined using real-time PCR and normalized to HPRT. Data are expressed as relative changes (fold) compared to uninfected lymph nodes, which were normalized to 1.

fold change difference in IL-10 induction between IP-10 and wild type infected mice at day 35 post infection. These results showed a higher expression of IL-10 in mice infected with IP-10 transgenic parasites compared to wild type infected mice. The opposite was found for IFN-γ in the ear model of infection. Higher IFN-γ was found in wild type infected mice at day 42 post infection with a much lower expression in the IP-10 infected mice. This might explain the fact that C57BL/6 mice start controlling *L. major* infection at day 42 in the ear model (Fig 4B). IL-4 was not detected in lymph nodes from IP-10 infected mice, which indicates that the hypervirulent phenotype shown in mice infected with IP-10 parasites is not due to an excessive Th2 immune response. The hypervirulent phenotype might be the result of the accumulation of higher numbers of $Foxp3^+$ $IL\text{-}10^+$ cells with a lower IFN-γ expression at the lesion sites and draining lymph nodes. These $Foxp3^+$cells might use an IL-10 dependent mechanism to downregulate Th1 immune response which could explain larger lesions observed in IP-10 infected mice. IL-10 has been shown to play a crucial role in the failure of the infected host to clear *L. major* infection. There is a balance between IL-10 and IFN-γ producing cells at the ears and lymph nodes of infected mice. This balance might be modified in the presence of IP-10 secreting parasites which could skew the immune response towards immunosuppression and an enhanced survival of the parasite.

Natural regulatory T cells might also be retained for longer periods at the lesion sites and draining lymph nodes in mice infected with IP-10 secreting parasites. It is plausible that these regulatory T cells are actively recruited or retained by their

expression of CXCR3 receptor. We have shown higher expression of CXCR3 receptor in lymph nodes from mice infected with IP-10 transgenic parasites in spite of similar numbers of activated T cells in both infected groups. Lymph nodes from IP-10 infected mice have also higher numbers of $Foxp3^+$ cells and $IL\text{-}10^+$ cells. This could suggest that *L. major* parasites that secrete IP-10 could recruit Foxp3 expressing regulatory T cells by their CXCR3 receptor. These cells express IL-10 and could employ this immunosuppressive cytokine to aid parasite survival. This suggests a novel mechanism developed by the parasite to evade the host response and manipulate cells of the adaptive immunity for their benefit.

APPENDIX 1: GENERATION OF VIRULENCE PROTEIN A (VAP-A) TRANSGENIC LEISHMANIA MAJOR.

Leishmania major enters macrophages silently and fails to engage toll like receptors. *L. major* fails to induce TNF-α, IL-12 or nitric oxide and therefore can not activate macrophages (14). In contrast, the intracellular bacteria, *Rhodococcus equi*, can induce cytokine production and activate macrophages. *Rhodococcus equi* express a molecule called virulence protein A (VapA) that has previously been shown to be a TLR-2 agonist (47). We wanted to generate *L. major* transgenic parasites that can activate the toll like receptor (TLR) pathway to examine a new macrophage activation mechanism. Activated macrophages release a wide array of mediators including reactive oxygen and nitrogen species, hydrolytic enzymes, bioactive lipids, and cytokines such as tumor necrosis factor alpha (TNF-α). These mediators are important for the killing of intracellular pathogens. We generated transgenic parasites that express VapA in their surface. We hypothesized that transgenic parasites expressing VapA would ligate TLR2 in macrophages and subsequently induce the production of TNF-α and nitric oxide. These parasites were engineered using a technique called Gene Splicing by Overlapping Extension PCR (SOE-PCR). In SOE-PCR, three different PCR products were created in separate PCR reactions and used together as templates to generate a hybrid SOE PCR product (Fig 22A). Activation of macrophages by VapA transgenic parasites was examined by measuring TNF-α and nitric oxide production.

Transgenic parasites express VapA mRNA and protein.

RNA was extracted from two different VapA transgenic clones to confirm their VapA mRNA expression. Transgenic parasites expressed VapA mRNA. No expression was detected in wild type parasites as expected (Fig 20A). In addition, VapA protein expression in transgenic parasites was detected by Western Blotting (Fig 20B).

VapA transgenic parasites failed to induce TNF-α production.

Bone marrow derived macrophages (BMMΦ) were primed with IFN-γ for 16 hours and subsequently stimulated with LPS or infected with different rations of wild type or VapA transgenic parasites. Supernatants were collected 24, 48 and 72 hours post infection and TNF-α concentrations were determined by ELISA. VapA transgenic parasites were not able to induce TNF-α production in infected BMMΦ at any given multiplicity of infection (MOI) (Fig 21A). They behaved similarly to wild type parasites which were also unable to induce TNF-α production. In contrast, LPS or rVapA stimulated cells induced high levels of TNF-α. These results suggest that VapA transgenic parasites were not able to ligate TLR-2. We know that transgenic parasites express VapA but we did not assess whether VapA expression was confined to the surface of the parasite or not. Expression of foreign genes in *Leishmania* is challenging and we can not be sure that proteins are expressed correctly. VapA could have been folded differently and therefore would have been unable to ligate TLR2.

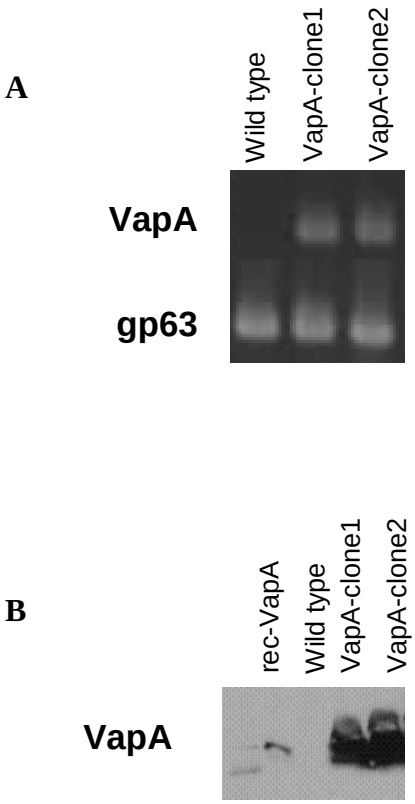

Fig 20. Transgenic parasites express VapA

Total RNA was isolated from wild-type and transgenic VapA parasites during promastigote development. VapA was amplified from the cDNA of transgenic parasites, but not from the cDNA of wild-type *L. major*. The gene gp63 was amplified from the cDNA as a loading control. (B) Equal amounts of whole parasites lysates were subject to electrophoresis on 15% SDS-PAGE and VapA protein expression was detected by Western Blotting.

VapA transgenic parasites failed to induce nitric oxide

Nitric oxide (NO) is a key immune mediator that is produced by activated macrophages. We measured NO production in cells infected with wild type or VapA transgenic parasites. Bone marrow derived macrophages (BMMΦ) were primed with IFN-γ for 16 hours and subsequently stimulated with LPS or infected with live, heat killed parasites and parasites opsonized with C5 deficient serum. Supernatants were collected 24, 48 and 72 hours post infection and NO production was determined. VapA transgenic parasites were unable to induce NO production in macrophages and behaved similarly to wild type parasites (Fig 21B). In contrast, LPS stimulated macrophages induced high NO production. These results along with the previous experiment suggest that VapA transgenic parasites do not activate macrophages in vitro. It is possible that VapA expression is flawed which impede proper ligation with TLR. Another possibility might be that transgenic parasites do not express VapA at their surface and therefore can not serve as TLR agonist. We can only conclude that these VapA transgenic parasites were no able to activate macrophages.

A

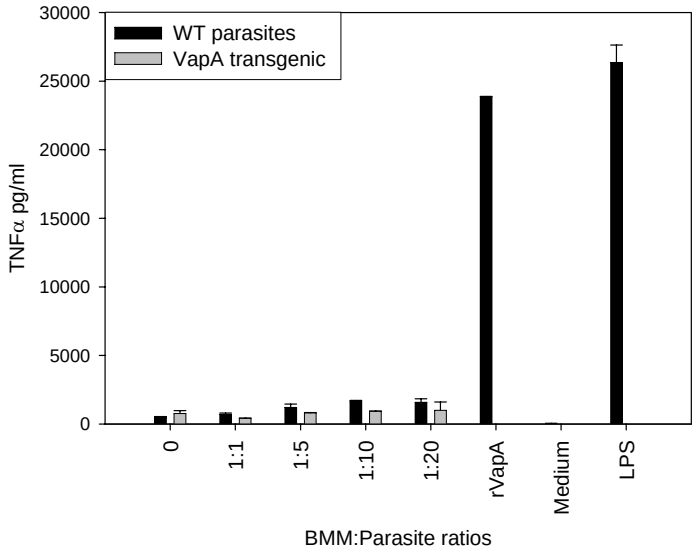

B

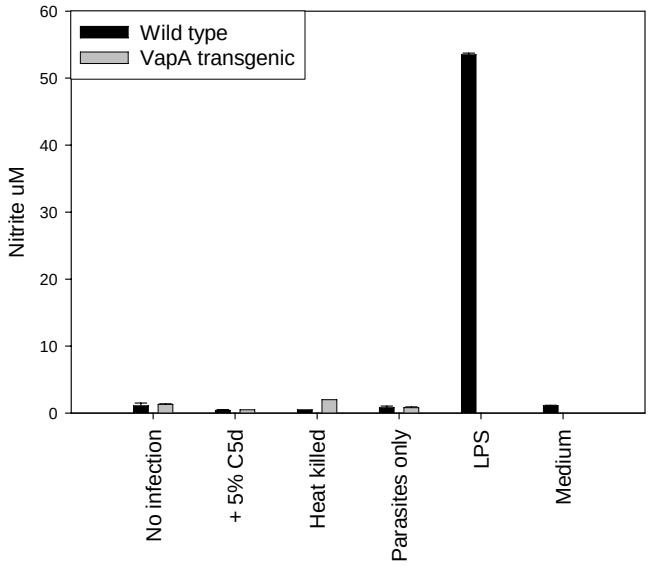

Fig 21 VapA transgenic parasites fail to activate macrophages

(A) BMMΦ were primed with 100 U/ml IFN-γ for 16 hours. Macrophages were either stimulated with 10 ng/ml LPS (*E. coli* 0127:B8 Sigma, St. Louis, MO) or infected wild type or VapA transgenic parasites. Supernatants were collected 48 hours post infection and TNF-α concentrations were determined by ELISA. (B) Griess reagent was added 1:1 (v:v) to culture supernatants and nitrite content was calculated by comparison to a sodium nitrite standard curve by measuring the absorbance at 550mn.

Material and Methods

Gene Splicing by Overlapping Extension (SOE) PCR

Three different PCR products were created in separate PCR reactions and used to generate a hybrid SOE PCR product that begins with a 5'-*SmaI* restriction site followed by the *L. major* gp63 signal sequence, the 564 bp of the *Rhodococcus equi* Vap A gene and ends the *L. major* GPI anchor sequence with a 3'- *XbaI* site.

The first PCR reaction generated a 123 basepair (bp) PCR product that contained a 5'-*SmaI* restriction site followed by the *L. major* gp63 signal sequence and a short sequence corresponding to the VapA gene. This fragment was created using the following primers: sense 5'-TTCCCGGGATGTCCGTCGA - 3' and antisense 5'-TGAAGAGTCTTGGCGTGTGCCCA -3'. These primers were used along with a plasmid template that contained the entire *L. major* gp63 gene (accession #: Y00647). After the gp63 PCR #1 product was generated, it was gel purified using a gel extraction kit (Qiagen, Valencia, CA). The second PCR reaction generated a 564 bp PCR product that contains the *Rhodococcus equi* Vap A gene, followed by a short sequence corresponding to the GPI anchor sequence of *L. major*. This fragment was created using the following primers: sense 5'-ACACGCCAAGACTCTTCACAAGACG - 3' and antisense 5'-CTGAGGCCGGCGTTGTGC -3'. After the VapA PCR #2 product was generated, it was gel purified using a gel extraction kit (Qiagen, Valencia, CA). The third PCR reaction generated a 198 bp fragment containing the GPI anchor sequence of *L. major* and the sequence corresponding to *XbaI* restriction site, using the following primers:

sense 5'-AACGCCGGCCTCAGAGTTGAG- 3' and antisense 5'-TATTTCTAGACTAGAGCGCCACGGCC -3'. The hybrid PCR product VapA-SOE was generated with two series of PCR reactions using gp63 PCR #1, VapA PCR #2 and GPI PCR #3 as templates (Fig 22A). The final PCR product was purified using a PCR purification kit (Qiagen) and ligated into the TA cloning vector, pCRII (Invitrogen).

The hybrid PCR product was excised from the TA cloning vector with *SmaI and XbaI*, gel purified, and ligated into the multiple cloning site of the *Leishmania* expression plasmid, pIR1SAT, which was generously provided by Dr. Steven Beverley (Washington University, St. Louis, MO) (Fig 22B). The ligated expression plasmid, pIR1SAT-IP-10 was transformed into Max Efficiency DH10B competent cells (Invitrogen) by heat-shock method. The pIR1SAT-IP-10 plasmid was isolated from DH10B cells using a plasmid maxi kit (Qiagen), digested with *SwaI*, and transfected into *Leishmania* parasites to permit integration into the parasite genome.

Transfection of Leishmania

L. major parasites ($1x10^8$ parasites) were resuspended in 400 µl of electroporation buffer [21 mM HEPES (pH 7.5), 137 mM NaCl, 5 mM KCl, 0.7 mM Na_2PO_4, and 6 mM glucose]. This suspension was mixed with 5 µg of linearized pIR1SAT-IP-10, added to a 0.4 cm Gene Pulser cuvette (BIORAD, Hercules, CA), and electroporated

(0.5 kV, 0.5 μFd) using BIORAD's Gene Pulser II. The cuvette was put on ice for 10 minutes. Electroporated parasites were added to blood agar plates containing SAT.

RNA isolation

RNA was isolated from $1x10^8$ wild-type or transgenic *L. major* promastigote using Trizol RNA prep (Invitrogen). The RNA was converted to cDNA using the manufacturer's protocol. VapA was amplified from the cDNA samples using the following primers: sense 5'-AAGACTCTTCACAAGACGGTTTCTAA-3' and antisense 5'-GGCGTTGTGCCAGCTACCAGA-3'. gp63 was amplified using the following primers: sense 5'-ATCCTCACCGACGAGAAGCGCGAC-3' and antisense 5'-ACGGAGGCGACGTACAACACGAAG-3'.

Western blotting

Wild type and VapA transgenic parasites were lysed in ice-cold lysis buffer (100 mM Tris (pH 8), 2 mM EDTA, 100 mM NaCl, 1% Triton X-100 containing complete EDTA-free protease inhibitors from Roche Diagnostics, which included 5 mM sodium vanadate, 10 mM sodium fluoride, 10 mM β-glycerophosphate sodium, and 5 mM sodium pyrophosphate). Equal amounts of protein were loaded onto 15% SDS-polyacrylamide gels, and then transferred to polyvinylidene difluoride membranes. Membranes were incubated with primary Abs overnight at 4°C, washed, and incubated with secondary Ab with HRP conjugates. The specific protein bands were

visualized by using Lumi-LightPLUS chemiluminescent substrate (Roche Diagnostics).

Cytokine measurement

A total of 3 x 10^5 BMMΦ per well were plated overnight in 24-well plates. Cells were primed with 100 U/ml IFN-γ for 16 hours (47). Macrophages were either stimulated with 10 ng/ml LPS (*E. coli* 0127:B8 Sigma, St. Louis, MO) or infected wild type or VapA transgenic parasites between 1:1 to 1:20 macrophage : parasite ratios. Supernatants were collected 24, 48 and 72 hours post infection and TNF-α concentrations were determined by a sandwich ELISA using Ab pairs provided by BD Pharmingen (G281-2626 and MP6-XT3) according to the manufacturer's instructions.

Nitric Oxide Determination

A total of 3 x 10^5 BMMΦ per well were plated overnight in 24-well plates. Cells were primed with 100 U/ml IFN-γ for 16 hours. Macrophages were either stimulated with 10 ng/ml LPS (*E. coli* 0127:B8 Sigma, St. Louis, MO), or infected wild type and VapA transgenic parasites. Macrophages were also infected with opsonized parasites with 5% C5 deficient serum and heat killed parasites. Griess reagent was added 1:1 (v:v) to culture supernatants and nitrite content was calculated by comparison to a sodium nitrite standard curve by measuring the absorbance at 550mn as previously described (47).

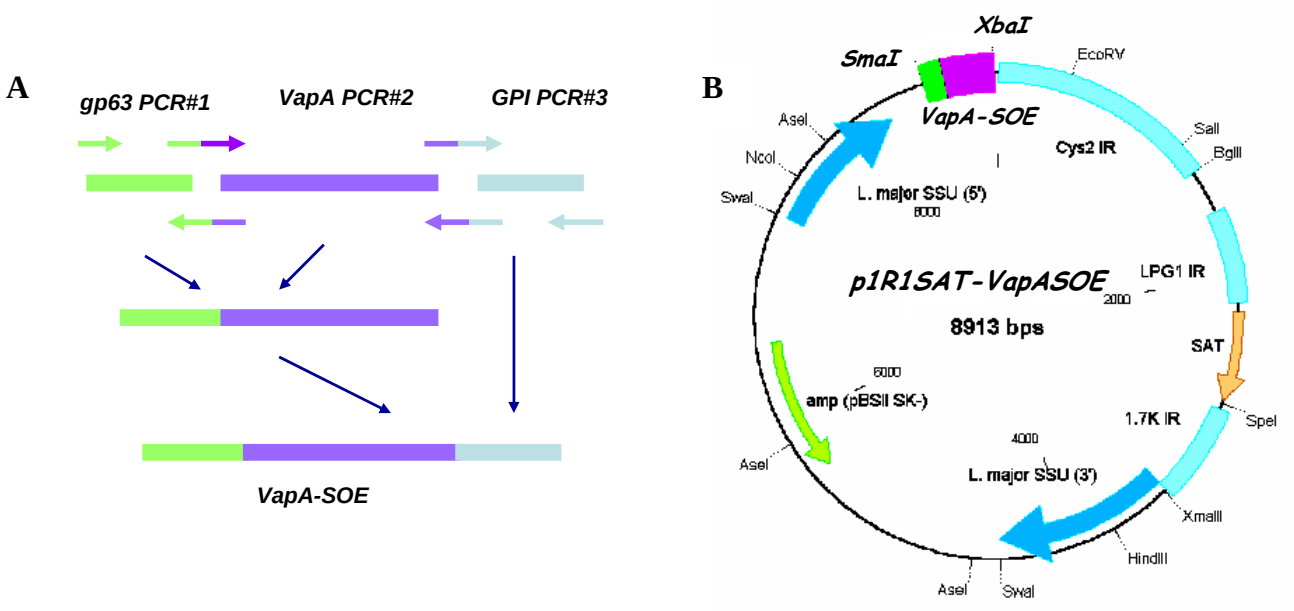

Figure 22. Gene Splicing by Overlaping Extension PCR and pIR1SAT-VapA.

(A) gp63 PCR#1, VapA PCR#2 and GPI PCR#3 were created in separate PCR reactions. PCR products were used together in a separate PCR reaction to create the hybrid PCR product. (B) P1R1SAT contains a multiple cloning site for insertion of the VapA-SOE hybrid product. The multiple cloning site is flanked by genes involved in transplicing and polyadenylation. The plasmid contains a streptothricin (SAT) resistance marker. The plasmid also contains the 5' and 3' portions of the *L. major* 18S ribosomal RNA subunit (SSU) for integration into the *Leishmania* genome**.**

APPENDIX 2: GREEN FLUORESCENT PROTEIN (GFP) EXPRESSING LEISHMANIA MEXICANA

Since its discovery, green fluorescent protein (GFP) (48) has been a useful biological marker applied extensively in molecular biology. GFP has found broad use in almost all organisms and all major cellular compartments. GFP has been used as a reporter gene, a cell marker and a fusion tag. We introduced a GFP gene into *Leishmania mexicana* genome to generate green parasites which can be used to visualized parasites in situ. Viable or fixed GFP expressing *Leishmania* can be directly visualized under the fluorescence microscope without cumbersome labeling procedures. Green fluorescent parasites were fixed with 4% paraformaldehyde onto a coverslip and *L mexicana* were visualized under fluorescent microscopy (Fig 23A). GFP parasites were also detected by flow cytometry (Fig 23B).

Generation of GFP transgenic parasites

A product that begins with a 5'-*SmaI* restriction site followed by 666 bp of the green fluorescent protein (GFP) gene and ends with a 3'-*XbaI* site was generated by PCR. This fragment was amplified from the pmaxGFP™ plamid from Amaxa Biosystems nucleofector kit as a template using the following primers: sense 5'-CCCCCGGGATGAAGATCGAGT - 3' and antisense 5'-GCTCTAGACTATGCGATCGGG-3'. A standard 50 ul reaction PCR using 45ul of Platinum PCR supermix (Invitrogen) with primers and the template was used to amplify GFP fragment according to the manufacture's protocol. The PCR product was purified using a PCR purification kit (Qiagen) and ligated into the TA cloning vector, pCRII (Invitrogen).

The PCR product was excised from the TA cloning vector with *SmaI – XbaI* double digestion, gel purified, and ligated into the multiple cloning site of the *Leishmania* expression plasmid, pIR1SAT. The ligated expression plasmid, pIR1SAT-GFP was transformed into Max Efficiency DH10B competent cells (Invitrogen) by Heat-shock method. The pIR1SAT-GFP plasmid was isolated from DH10B cells using a plasmid maxi kit (Qiagen), digested with *SwaI*, and transfected into *Leishmania* parasites to permit integration into the parasite genome. Transfection of *L. mexicana* parasites was performed as described above.

A

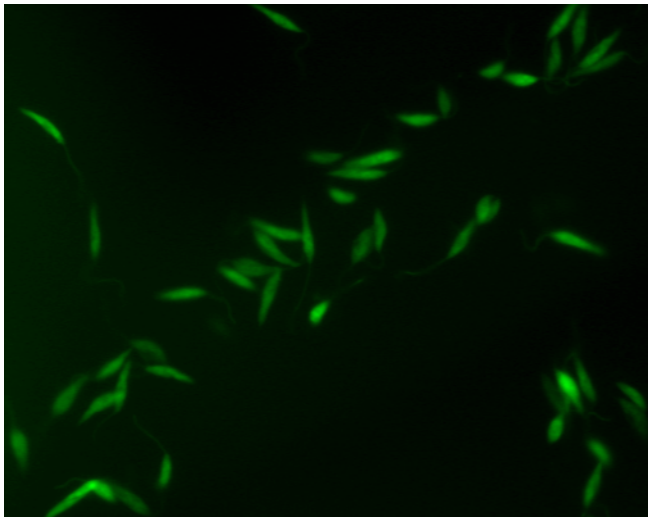

B

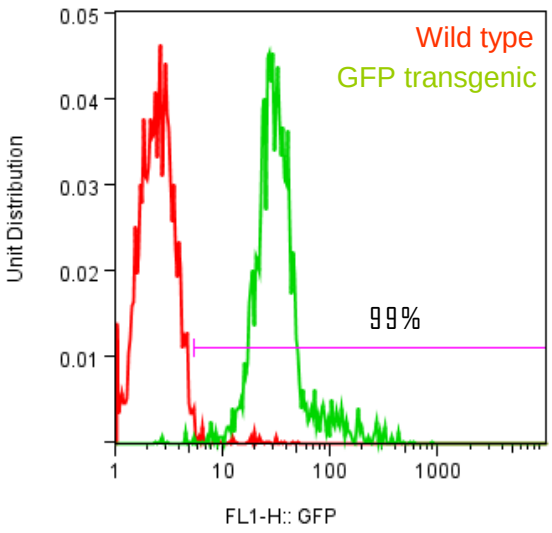

Fig 23 Green fluorescent protein expressing Leishmania mexicana

(A) GFP parasites were fixed with 4% paraformaldehyde and placed onto a cover slip. Parasites were visualized under fluorescent microscopy. (B) GFP parasites were detected by flow cytometry.

REFERENCES

1. Ilg,T. 2001. Lipophosphoglycan of the protozoan parasite Leishmania: stage- and species-specific importance for colonization of the sandfly vector, transmission and virulence to mammals. *Med. Microbiol. Immunol. (Berl)* 190:13-17.

2. http://www.who.int/leishmaniasis/burden/en/

3. Burchmore,R.J. and M.P.Barrett. 2001. Life in vacuoles--nutrient acquisition by Leishmania amastigotes. *Int. J. Parasitol.* 31:1311-1320.

4. Naderer T, Vince JE, McConville MJ. Surface determinants of Leishmania parasites and their role in infectivity in the mammalian host. Curr Mol Med. 2004 Sep;4(6):649-65

5. Sacks,D. and N.Noben-Trauth. 2002. The immunology of susceptibility and resistance to Leishmania major in mice. *Nat. Rev. Immunol.* 2:845-858.

6. Puentes, S.M., Da Silva, R.P., Sacks, D.L., Hammer, C.H. & Joiner, K.A. Serum resistance of metacyclic stage *Leishmania major* promastigotes is due to release of C5b-9. *J. Immunol.* 145, 4311−4316 (1990).

7. Wozencraft AO, Blackwell JM. Increased infectivity of stationary-phase promastigotes of Leishmania donovani: correlation with enhanced C3 binding capacity and CR3-mediated attachment to host macrophages. Immunology 1987;60:559–563.

8. Mosser, D.M. & Edelson, P.J. The mouse macrophage receptor for C3bi (CR3) is a major mechanism in the phagocytosis of *Leishmania* promastigotes. *J. Immunol.* 135, 2785−2789 (1985).

9. van Zandbergen G, et al. Cutting edge: neutrophil granulocyte serves as a vector for Leishmania entry into macrophages. J Immunol 2004;173:6521–6525.

10. Desjardins, M. and Descoteaux, A. (1997) Inhibition of phagolysosomal biogenesis by the *Leishmania l*ipophosphoglycan. *J. Exp. Med.* 185, 2061–2068.

11. Sorensen, A.L. *et al.* (1994) *Leishmania major* surface protease gp63 interferes with the function of human monocytes and neutrophils *in vitro*. *Acta Pathol. Microbiol. Immunol. Scand.* 102, 265–271.

12. Moore, K.J., Labrecque, S. & Matlashewski, G. Alteration of *Leishmania donovani* infection levels by selective impairment of macrophage signal transduction. *J. Immunol.* 150, 4457−4465 (1993).

13. Reiner,N.E., W.Ng, and W.R.McMaster. 1987. Parasite-accessory cell interactions in murine leishmaniasis. II. Leishmania donovani suppresses macrophage expression of class I and class II major histocompatibility complex gene products. *J. Immunol.* 138:1926-1932.

14. McDowell, M.A. & Sacks, D.L. Inhibition of host cell signal transduction by *Leishmania*: observations relevant to the selective impairment of IL-12 responses. *Curr. Opin. Microbiol.* 2, 438−443 (1999).

15. Nandan, D. & Reiner, N.E. Attenuation of γinterferon-induced tyrosine phosphorylation in mononuclear phagocytes infected with *Leishmania donovani*: selective inhibition of signaling through Janus kinases and Stat1. *Infect. Immun.* 63, 4495−4500 (1995).

16. Belkaid Y, Piccirillo CA, Mendez S, Shevach EM, Sacks DL. CD4+CD25+ regulatory T cells control Leishmania major persistence and immunity. Nature. 2002 Dec 5;420(6915):502-7.

17. Robertson, M. J. 2002. Role of chemokines in the biology of natural killer cells. J. Leukoc. Biol. 71:173-183.

18. Sanchez J, Moldobaeva A, McClintock J, Jenkins J, Wagner EM. The role of CXCR2 in systemic neovascularization of the mouse lung. J Appl Physiol.2007 Jun 7.

19. Charo, I.F., and R.M. Ransohoff. 2006. The many roles of chemokines and chemokine receptors in inflammation. *N. Engl. J. Med.* 354:610–621.

20. B. Moser *et al.*, Chemokines: multiple levels of leukocyte migration control, *Trends Immunol.* 25 (2004), pp. 75–84.

21. Ritter, U., H.Moll, T. Laskay, E. Brocker, O. Velazco, I. Becker, and R. Gillitzer. 1996. Differential expression of chemokines in patients with localized and diffuse cutaneous American leishmaniasis. J. Infect. Dis. 173:699-709.

22. Conrad SM, Strauss-Ayali D, Field AE, Mack M, Mosser DM. Leishmania-derived murine monocyte chemoattractant protein 1 enhances the recruitment of a restrictive population of CC chemokinechemokine receptor 2-positive macrophages. Infect Immun. 2007 Feb;75(2):653-65.

23. Steigerwald M, Moll H. *Leishmania major* modulates chemokine and chemokine receptor expression by dendritic cells and affects their migratory capacity. Infect Immun. 2005 Apr;73(4):2564-7.

24. Mohan, K., E. Cordeiro, M. Vaci, C. McMaster, and T. B. Issekutz. 2005. CXCR3 is required for migration to dermal inflammation by normal and in vivo activated T

cells: differential requirements by CD4 and CD8 memory subsets. Eur. J. Immunol. 35:1702-1711.

25. Rosas, L. E., J. Barbi, B. Lu, Y. Fujiwara, C. Gerard, V. M. Sanders, and A. R. Satoskar. 2005. CXCR3-/- mice mount an efficient Th1 response but fail to control *Leishmania major* infection. Eur. J. Immunol. 35:515-523.

26. Zaph, C., and P. Scott. 2003. Interleukin-12 regulates chemokine gene expression during the early immune response to *Leishmania major*. Infect. Immun. 71:1587-1589.

27. Vester, B., Muller, K., Solbach, W., Laskay, T. (1999) Infect. Immun. 67, 3155-9.

28. Yurchenko E, Tritt M, Hay V, Shevach EM, Belkaid Y, Piccirillo CA. CCR5-dependent homing of naturally occurring CD4+ regulatory T cells to sites of Leishmania major infection favors pathogen persistence. J Exp Med. 2006 Oct 30;203(11):2451-60.

29. Vasquez RE, Soong L. CXCL10/gamma interferon-inducible protein 10-mediated protection against Leishmania amazonensis infection in mice. Infect Immun. 2006 Dec;74(12):6769-77.

30. Hailu A, van der Poll T, Berhe N, Kager PA. Elevated plasma levels of interferon (IFN)-gamma, IFN-gamma inducing cytokines, and IFN-gamma inducible CXC chemokines in visceral leishmaniasis. Am J Trop Med Hyg. 2004 Nov;71(5):561-7.

31. Sugiyama,H., R.Gyulai, E.Toichi, E.Garaczi, S.Shimada, S.R.Stevens, T.S.McCormick, and K.D.Cooper. 2005. Dysfunctional blood and target tissue CD4+CD25high regulatory T cells in psoriasis: mechanism underlying unrestrained pathogenic effector T cell proliferation. *J. Immunol.* 174:164-173.

32. Mills KH, McGuirk P. Antigen-specific regulatory T cells--their induction and role in infection. Semin Immunol. 2004 Apr;16(2):107-17. Review.

33. Sakaguchi S , et al. Foxp3^{+}CD25^{+}CD4^{+} natural regulatory T cells in dominant self-tolerance and autoimmune disease. Immunol Rev 2006; 212: 8– 27.

34. Roncarolo MG , et al. Interleukin-10-secreting type 1 regulatory T cells in rodents and humans. Immunol Rev 2006; 212: 28– 50.

35. Lu L, Werneck MBF, Cantor H . The immunoregulatory effects of Qa-1. Immunol Rev 2006; 212: 51– 59.

36. Fontenot JD, Rasmussen JP, Williams LM, Dooley JL, Farr AG, Rudensky AY. Regulatory T cell lineage specification by the forkhead transcription factor foxp3. Immunity. 2005 Mar;22(3):329-41.

37. Kursar M, Koch M, Mittrücker HW, Nouailles G, Bonhagen K, Kamradt T, Kaufmann SH. Cutting Edge: Regulatory T cells prevent efficient clearance of Mycobacterium tuberculosis. J Immunol. 2007 Mar 1;178(5):2661-5.

38. Hisaeda H, Maekawa Y, Iwakawa D, Okada H, Himeno K, Kishihara K, Tsukumo S, Yasutomo K. Escape of malaria parasites from host immunity requires CD4+ CD25+ regulatory T cells. Nat Med. 2004 Jan;10(1):29-30.

39. Ji J, Masterson J, Sun J, Soong L. CD4+CD25+ regulatory T cells restrain pathogenic responses during Leishmania amazonensis infection. J Immunol. 2005 Jun 1;174(11):7147-53.

40. Mendez S, Reckling SK, Piccirillo CA, Sacks D, Belkaid Y. Role for CD4+ CD25+ regulatory T cells in reactivation of persistent leishmaniasis and control of concomitant immunity. J Exp Med 2004;200:201–210.

41. Suffia I, Reckling SK, Salay G, Belkaid Y. A role for CD103 in the retention of CD4+CD25+ Treg and control of Leishmania major infection. J Immunol 2005;174:5444–5455.

42. Robinson PW, Green SJ, Carter C, Coadwell J, Kilshaw PJ. Studies on transcriptional regulation of the mucosal T-cell integrin alphaEbeta7 (CD103). Immunology 2001;103:146–154.

43. Suffia IJ, Reckling SK, Piccirillo CA, Goldszmid RS, Belkaid Y. Infected site-restricted Foxp3+ natural regulatory T cells are specific for microbial antigens. J Exp Med. 2006 Mar 20;203(3):777-88.

44. Afonso,L.C. and P.Scott. 1993. Immune responses associated with susceptibility of C57BL/10 mice to Leishmania amazonensis. *Infect. Immun.* 61:2952-2959.

45. Belkaid,Y., K.F.Hoffmann, S.Mendez, S.Kamhawi, M.C.Udey, T.A.Wynn, and D.L.Sacks. 2001. The role of interleukin (IL)-10 in the persistence of Leishmania major in the skin after healing and the therapeutic potential of anti-IL-10 receptor antibody for sterile cure. *J. Exp. Med.* 194:1497-1506.

46. Belkaid Y, Mendez S, Lira R, Kadambi N, Milon G, Sacks D. A natural model of Leishmania major infection reveals a prolonged "silent" phase of parasite amplification in the skin before the onset of lesion formation and immunity. J Immunol. 2000 Jul 15;165(2):969-77.

47. Darrah PA, Monaco MC, Jain S, Hondalus MK, Golenbock DT, Mosser DM. Innate immune responses to Rhodococcus equi. J Immunol. 2004 Aug ;173(3):1914-24.

48. Shimomura O, Johnson FH, Saiga Y. Extraction, purification and properties of aequorin, a bioluminescent protein from the luminous hydromedusan, Aequorea. J Cell Comp Physiol. 1962 Jun;59:223-39.